20 μmol/L DMPP both induced G2/M cell cycle block, while 20 μmol/L TMPP additionally induced apoptosis in leukemia cells. Moreover, TMPP treatment induced a decrease in cell cycle progression signals, tumor cell survival, and led to the activation of caspase-3 and -9.

FoxM1 is a transcription factor that regulates proliferation and cell cycle progression. Recently, it has been reported that FoxM1 promotes cell cycle progression by downregulation $p27^{Kip1}$ via multiple mechanisms [23]. We also have reported previously that overexpression of FoxM1 regulates the proliferation of leukemia cells, suggesting a potential mechanism for cell cycle progression in leukemia cells (in press). In current leukemia therapy, however, there are no effective antileukemic agents which target transcription factors.

Surprisingly, we found that TMPP/DMPP suppressed FoxM1 expression in leukemia cells. Although information regarding the effect of FoxM1 down-regulation in leukemia cells is scarce, we found that reducing FoxM1 expression resulted in both the inhibition of leukemia cell proliferation and an increase in the population of leukemia cells at G2/M phase 7 days after transfection compared to control siRNA-transfected cells and untreated cells. In contrast, overexpression of FoxM1 promoted the proliferation of leukemia cells. These data are consistent with the notion that FoxM1 protein is a key regulator of G2/M progression and is activated in many human malignancies [23–29]. Further, we showed that FoxM1 reduction not only increased the expression of $p27^{Kip1}$ and $p21^{Cip1}$ proteins, but also decreased that of Cdc25B, Cyclin D1, Cyclin A, KIS, and Aurora-B kinase proteins. Further, the decrease in expression of Cdc25B, Cyclin D1, Cyclin B, KIS, and Aurora-B kinase and the increase in expression of $p27^{Kip1}$ and $p21^{Cip1}$ proteins were strongly correlated with the altered cell cycle distribution and leukemia cell growth suppression. These results suggest that FoxM1 affects the leukemia cell cycle by regulating the expression levels of these proteins and may represent for a potential target for TMPP treatment.

FoxM1 has been reported to affect both the G1-S and G2-M transitions in the cell cycle [30]. G1-S transition is promoted by suppression of CDKIs such as $p27^{Kip1}$ brought on by inducing expression of KIS and Cyclin D1. G2-M transition is promoted via suppression of CDKIs such as $p21^{Cip1}$ brought on by inducing expression of Cdc25B, Cyclin A, and Aurora-B kinase. In the present study, treatment with low concentrations of TMPP and DMPP resulted in an increase in the distribution of G2/M, but not G1, leukemia cells, and no increase in the population of apoptotic cells. On western blot analysis, we found a greater reduction in levels of Cdc25B, Cyclin A, and $p21^{Cip1}$, which relate to the G2-M transition process, than in those of KIS, Cyclin D1, and $p27^{Kip1}$, which relate to the G1-S transition process. These results may suggest the mechanisms of the increase of G2/M distribution.

Further, TMPP was shown to act on expression of several key cell cycle proteins to cause arrest or apoptosis in a dose-dependent manner. Several studies have found that expression of $p21^{Cip1}$ causes strong G2 arrest and induces resumption of leukemia cell cycle progression [31, 32]. In leukemia cells, there is a strong correlation between the expression of Cyclin D1 and $p21^{Cip1}$, which reflects a complicated network regulating the proliferation and differentiation of these cells [33]. Aurora-B kinase has been reported to be aberrantly expressed in several human leukemia cell lines (n=15, e.g. PALL-1, PALL-2, HL-60, NB4, MV4-11, etc) as well as in freshly isolated leukemia cells from individuals with AML (n=44) [34]. Here, we found that TMPP treatment at low concentration reduced Aurora-B kinase expression in leukemia cells. At high concentration, TMPP induced apoptosis of leukemia cells via the caspase pathway. These results suggest that TMPP induced an increase in the G2/M cell population at a low concentration and an increase in apoptotic cells at a high concentration in leukemia cells.

The cytotoxic effects of TMPP on the cell lines above were also seen in clinical AML specimens derived from AML patients. The viability of AML cells was significantly reduced at TMPP concentrations greater than 4 μmol/L, whereas the viability of normal $ALDH^{hi}$ cells was only slightly reduced with TMPP administration in a dose-dependent manner. Levels of CFU-GEMM (colony forming unit-granulocyte, erythroid, macrophage, megakaryocyte), CFU-GM (colony forming unit-granulocyte, macrophage) and BFU-E (burst forming unit-erythroid) derived from normal progenitor cells were moderately reduced on treatment with TMPP compared to untreated cells (data not shown). Moreover, we observed that FoxM1 mRNA was overexpressed in acute leukemia specimens, and treatment with TMPP reduced the expression of FoxM1 mRNA an AML cells. Taken together, these data indicate that inhibition of FoxM1 represents an attractive target for leukemia therapy.

In conclusion, we synthesized two deoxybromophospha sugar derivatives, TMPP and DMPP, and found that these agents are potent inhibitors of FoxM1, inducing G2/M cell cycle block via down-regulation of FoxM1 at low concentrations, and apoptosis via the caspase pathway at high concentrations *in vitro*. FoxM1 has therefore been characterized as a target molecule of TMPP in leukemia cells. Further, TMPP significantly reduced AML cell viability in clinical specimens derived from AML patients, but not in normal hematopoietic progenitor cells. These results suggest that TMPP may efficiently inhibit cell cycle and induce apoptosis, and thereby facilitate the development of new strategies in targeted antileukemic therapy.

Acknowledgements This study was supported by Ministry of Education, Culture, Sports Science and Technology of Japan, Aid for Scientific Research (#17590987).

References

1. Witkowski JT, Robins RK, Sidwell RW, Simon LN (1972) Design, synthesis, and broad spectrum antiviral activity of 1-β-D-ribofuranosyl-1, 2, 4-triazole-3-carboxamide and related nucleosides. J Med Chem 15:1150–1154. doi:10.1021/jm00281a014
2. Mitsuya H, Weinhold KJ, Furman PA, St Clair MH, Lehrman SN, Gallo RC, Bolognesi D, Barry DW, Broder S (1985) 3'-Azido-3'-deoxythymidine (BW A509U); an antiviral agent that inhibits the infectivity and cytopathic effect of human T-lymphotropic virus type III/lymphadenopathy-associated virus in vitro. Proc Natl Acad Sci USA 82:7096–7100. doi:10.1073/pnas.82.20.7096
3. McGuigan C, Pathirana RN, Balzarini J, De Clercq E (1993) Intracellular delivery of bioactive AZT nucleotides by aryl phosphate derivatives of AZT. J Med Chem 36:1048–1052. doi:10.1021/jm00060a013
4. Legler G, Julich E (1984) Synthesis of 5-amino-5-deoxy-D-mannopyranose and 1, 5-dideoxy-1, 5-imino-D-mannitol, and inhibition of alpha- and beta-D-mannosidases. Carbohydr Res 128:61–72. doi:10.1016/0008-6215(84)85084-3
5. Takayama S, Martin R, Wu J, Laslo K, Siuzdak G, Wong CH (1997) Chemoenzymic preparation of novel cyclic imine sugars and rapid biological activity evaluation using electrospray mass spectrometry and kinetic analysis. J Am Chem Soc 119:8146–8151. doi:10.1021/ja971695f
6. Davis BG, Maughan MA, Chapman TM, Villard R, Courtney S (2002) Novel cyclic sugar imines: carbohydrate mimics and easily elaborated scaffold for aza-sugars. Org Lett 4:103–106. doi:10.1021/ol016970o
7. Sinskey AJ, Barbas CF, Pederson RL, Wang YF, Wong CH (1989) Use of a recombinant bacterial fructose-1, 6-diphosphate aldolase in aldol reactions: preparative syntheses of 1-deoxynojirimycin, 1-deoxymannojirimycin, 1, 4-dideoxy-1, 4-imino-D-arabinitol, and fagomine. J Am Chem Soc 111:3924–3927. doi:10.1021/ja00193a025
8. Braanalt J, Kvarnstroem I, Niklasson G, Svensson SCT, Classon B, Samuelsson B (1994) Synthesis of 2', 3'-Dideoxy-3'-C-(hydroxymethyl)-4'-thionucleosides as potential inhibitors of HIV. J Org Chem 59:1783–1788. doi:10.1021/jo00086a032
9. Chmielewski M, Whistler RL (1975) 5-Thio-D-fructofuranose. J Org Chem 40:639–643. doi:10.1021/jo00893a021
10. Wang P, Agrofoglio LA, Newton MG, Chu CK (1999) Chiral synthesis of carbocyclic analogues of L-ribofuranosides. J Org Chem 64:4173–4178. doi:10.1021/jo9812330
11. Biggadike K, Borthwick AD, Exall AM (1990) Short convergent route to chiral pyrimidine analogs of 2'-deoxyneplanocin. Am J Chem Soc 6:458–459
12. Inouye S, Tsuruoka T, Ito T, Niida T (1968) Structure and synthesis of nojirimycin. Tetrahedron 24:2125–2144. doi:10.1016/0040-4020(68)88115-3
13. Karpas A, Fleet GW, Dwek RA, Petursson S, Namgoong SK, Ramsden NG, Jacob GS, Rademacher TW (1988) Aminosugar derivatives as potential anti-human immunodeficiency virus agents. Proc Natl Acad Sci USA 85:9229–9233. doi:10.1073/pnas.85.23.9229
14. Goss PE, Baker MA, Carver JP, Dennis JW (1995) Inhibitors of carbohydrate processing: a new class of anticancer agents. Clin Cancer Res 1:935–944
15. Yamashita M, Nakatsukasa Y, Yoshikane M, Yoshida H, Ogata T, Inokawa S (1977) A novel method for the synthesis of sugar derivatives containing a phosphorus atom in the hemiacetal ring. Carbohydr Res 59:12–14. doi:10.1016/S0008-6215(00)83321-2
16. Yamashita M, Nakatsukasa Y, Yoshida H, Tsunekawa K, Oshikawa T, Seo K (1979) Synthesis of 5, 6-dideoxy-3-O-methyl-5-C-(phenylphosphinyl)-D-glucopyranose and its 1, 2, 4-triacetate. Carbohydr Res 70:247–261. doi:10.1016/S0008-6215(00)87105-0
17. Yamashita M, Yamada M, Tsunekawa K, Oshikawa T, Seo K, Inokawa S (1983) Synthesis of 5-deoxy-3-O-methyl-5-C-(phenylphosphinyl)-L-idopyranose. Carbohydr Res 121:4–5. doi:10.1016/0008-6215(83)84034-8
18. Yamashita M, Yamada M, Sugiura M, Nomoto H, Oshikawa T (1987) Functional group interconversion of a nitro group of phosphorus compounds and synthesis of some phosphino sugars. J Chem Soc Jpn 7:1207–1213
19. Bennet JM, Daniel MT (1985) Proposed revised criteria for the classification of acute myeloid leukemia: a report of the French-British-American cooperative group. Ann Intern Med 103:620–625
20. Dimberg A, Bahram F, Karlberg I, Larsson LG, Nilsson K, Oberg F (2002) Retinoic acid-induced cell cycle arrest of human myeloid leukemia cell lines is associated with sequential down-regulation of c-Myc and cyclin E and posttranscriptional upregulation of p27 (kip1). Blood 99:2199–2206. doi:10.1182/blood.V99.6.2199
21. Petrovic V, Costa RH, Lau LF, Raychaudhuri P, Tyner AL (2008) FoxM1 regulates growth factor induced expression of the KIS kinase to promote cell cycle progression. J Biol Chem 104:453–460
22. Hess DA, Meyerrose TE, Wirthlin L, Craft TP, Herrbrich PE, Creer MH, Nolta JA (2004) Functional characterization of highly purified human hematopoietic repopulating cells isolated according to aldehyde dehydrogenase activity. Blood 104:1648–1655. doi:10.1182/blood-2004-02-0448
23. Ye H, Holterman AX, Yoo KW, Franks RR, Costa RH (1999) Premature expression of the winged helix transcription factor HFH-11B in regenerating mouse liver accelerates hepatocyte entry into S-phase. Mol Cell Biol 19:8570–8580
24. Wang X, Kiyokawa H, Dennewitz MB, Costa RH (2002) The Forkhead Box m1b transcription factor is essential for hepatocyte DNA replication and mitosis during mouse liver regeneration. Proc Natl Acad Sci USA 99:16881–16886. doi:10.1073/pnas.252570299
25. Korver W, Schilham MW, Moerer P, van den Hoff MJ, Dam K, Lamers WH, Medema RH, Clevers H (1998) Uncoupling of S phase and mitosis in cardiomyocytes and hepatocytes lacking the winged-helix transcription factor. Trident Curr Boil 8:1327–1330. doi:10.1016/S0960-9822(07)00563-5
26. Laoukili J, Kooistra MR, Brás A, Kauw J, Kerkhoven RM, Morrison A, Clevers H, Medema RH (2005) FoxM1 is required for execution of the mitotic programme and chromosome stability. Nat Cell Biol 7:126–136. doi:10.1038/ncb1217
27. Wonsey DR, Follettie MT (2005) Loss of the forkhead transcription factor FoxM1 causes centrosome amplification and mitotic catastrophe. Cancer Res 65:5181–5189. doi:10.1158/0008-5472.CAN-04-4059
28. Leung TW, Lin SS, Tsang AC, Tong CS, Ching JC, Leung WY, Gimlich R, Wong GG, Yao KM (2001) Over-expression of FoxM1 stimulates cyclin B1 expression. FEBS Lett 507:59–66. doi:10.1016/S0014-5793(01)02915-5
29. Yokozawa T, Towatari M, Iida H, Takeyama K, Tanimoto M, Kiyoi H, Motoji T, Asou N, Saito K, Takeuchi M, Kobayashi Y, Miyawaki S, Kodera Y, Ohno R, Saito H, Naoe T (2000) Prognostic significance of the cell cycle inhibitor p27Kip1 in acute myeloid leukemia. Leukemia 14:28–33. doi:10.1038/sj.leu.2401640
30. Wonsey D, Follettie MT (2005) Loss of the forkhead transcription factor FoxM1 causes centrosome amplification and mitotic catastrophe. Cancer Res 65:5181–5189. doi:10.1158/0008-5472.CAN-04-4059
31. Bunz F, Dutriaux A, Lengauer C, Waldman T, Zhou S, Brown JP, Sedivy JM, Kinzler KW, Vogelstein B (1998) Requirement for

p53 and p21 to sustain G2 arrest after DNA damage. Science 282:1497–1501. doi:10.1126/science.282.5393.1497
32. Williams ME, Swerdlow SH, Rosenberg CL, Arnold A (1993) Chromosome 11 translocation breakpoints at the PRAD1/cyclin D1 gene locus in centrocytic lymphoma. Leukemia 7:241–245
33. Zhang H, Kobayashi R, Galaktionov K, Beach D (1995) p19Skp1 and p45Skp2 are essential elements of the cyclin A-CDK2 S phase kinase. Cell 82:915–925. doi:10.1016/0092-8674(95)90271-6
34. Ikezoe T, Yang J, Nishioka C, Tasaka T, Taniguchi A, Kuwayama Y, Komatsu N, Bandobashi K, Togitani K, Koeffler HP, Taguchi H (2007) A novel treatment strategy targeting Aurora kinases in acute myelogenous leukemia. Mol Cancer Ther 6:1851–1859. doi:10.1158/1535-7163.MCT-07-0067

bjh research paper

CMC-544 (inotuzumab ozogamicin) shows less effect on multidrug resistant cells: analyses in cell lines and cells from patients with B-cell chronic lymphocytic leukaemia and lymphoma

Akihiro Takeshita,[1,2] Kaori Shinjo,[2] Nozomi Yamakage,[1] Takaaki Ono,[2] Isao Hirano,[2] Hirotaka Matsui,[2] Kazuyuki Shigeno,[2] Satoki Nakamura,[2] Tadasu Tobita,[3] Masato Maekawa,[1] Kazunori Ohnishi,[2] Yoshikazu Sugimoto,[4] Hitoshi Kiyoi,[5] Tomoki Naoe[5] and Ryuzo Ohno[6]

[1]Laboratory and [2]Internal Medicine, Hamamatsu University School of Medicine, Handayama, Higashiku, Hamamatsu, [3]Yaizu Shimin Hospital, Dohara, Yaizu, [4]Graduate School of Pharmaceutical Science, Keio University, Shibakoen, Minatoku, Tokyo, [5]Haematology and Oncology, Nagoya University School of Medicine, Tsurumai, Showaku, and [6]Aichi Cancer Centre, Kanokoden, Chikusaku, Nagoya, Japan

Received 26 December 2008; accepted for publication 17 March 2009

Correspondence: Akihiro Takeshita, Laboratory and Internal Medicine, Hamamatsu University School of Medicine, 1-20-1 Handayama, Higashiku, Hamamatsu 431-3192, Japan.
E-mail: akihirot@hama-med.ac.jp

Summary

The effect of CMC-544, a calicheamicin-conjugated anti-CD22 monoclonal antibody, was analysed in relation to CD22 and P-glycoprotein (P-gp) in B-cell chronic lymphocytic leukaemia (CLL) and non-Hodgkin lymphoma (NHL) *in vitro*. The cell lines used were CD22-positive parental Daudi and Raji, and their P-gp positive sublines, Daudi/MDR and Raji/MDR. Cells obtained from 19 patients with B-cell CLL or NHL were also used. The effect of CMC-544 was analysed by viable cell count, morphology, annexin-V staining, and cell cycle distribution. A dose-dependent, selective cytotoxic effect of CMC-544 was observed in cell lines that expressed CD22. CMC-544 was not effective on Daudi/MDR and Raji/MDR cells compared with their parental cells. The MDR modifiers, PSC833 and MS209, restored the cytotoxic effect of CMC-544 in P-gp-expressing sublines. In clinical samples, the cytotoxic effect of CMC-544 was inversely related to the amount of P-gp ($P = 0{\cdot}003$), and to intracellular rhodamine-123 accumulation ($P < 0{\cdot}001$). On the other hand, the effect positively correlated with the amount of CD22 ($P = 0{\cdot}010$). The effect of CMC-544 depends on the levels of CD22 and P-gp. Our findings will help to predict the clinical effectiveness of this drug on these B-cell malignancies, suggesting a beneficial effect with combined use of CMC-544 and MDR modifiers.

Keywords: CMC-544, monoclonal antibody, CD22, P-glycoprotein, calicheamicin.

Rituximab in combination with chemotherapy has been used to treat various subtypes of B cell malignancies including chronic lymphocytic leukaemia (B-CLL) and non-Hodgkin lymphoma (B-NHL) (Hiddemann *et al*, 2006; Montserrat *et al*, 2006; Coiffier, 2007; Fanale & Younes, 2007). However, a considerable number of patients are refractory to treatment with rituximab and relapse after demonstrating an initial response. Several prognostic factors have been reported (Auer *et al*, 2007; Bonavida, 2007). The refractory nature to treatment may be partly attributed to the development of multidrug resistance (MDR), involving a series of events by which malignant cells become resistant to several structurally unrelated agents for B cell malignancies (Svoboda-Beusan *et al*, 2000; Andreadis *et al*, 2007). To overcome this resistance, several new agents have been developed (Hiddemann *et al*, 2006). Among these, CMC-544 has been introduced as a promising agent for the treatment of refractory and resistant cases.

CMC-544, inotuzumab ozogamicin, is a conjugate of N-acetyl γ-calicheamicin dimethyl hydrazide (NAc γ-calicheamicin DMH) and a recombinant humanized antibody (IgG_4) directed against the CD22 antigen (DiJoseph *et al*, 2004, 2006, 2007). Calicheamicin, a very potent anti-tumour antibiotic agent, binds to the minor groove of DNA in a sequence-specific manner, and breaks double-stranded DNA by abstracting specific hydrogen atoms, which may be the initial step in cell damage (Zein *et al*, 1988).

Gemtuzumab ozogamicin (GO), another immunoconjugate of NAc γ-calicheamicin DMH, is targeted to the human CD33 antigen and has been widely utilized for the treatment of acute

First published online 20 April 2009
doi:10.1111/j.1365-2141.2009.07701.x

myeloid leukaemia (AML) (Larson *et al*, 2005). However, the clinical outcome after treatment with GO was negatively associated with drug resistance in AML (Naito *et al*, 2000; Matsui *et al*, 2002; Walter *et al*, 2007). These effects, which are closely related to the expression of CD33 and P-glycoprotein (P-gp), have been reported by several investigators, including our laboratory (Naito *et al*, 2000; Matsui *et al*, 2002; Takeshita *et al*, 2005).

Thus, P-gp may also play a role in clinical resistance to CMC-544. If calicheamicin were pumped out by P-gp in the same manner as GO, CMC-544 would be less effective on B-CLL and NHL cells that express P-gp. This study investigated the cytotoxic effect of CMC-544 in relation to P-gp on cell lines and malignant cells from patients with B-CLL and NHL. Furthermore, other factors, such as level of CD22 and internalisation, were analysed regarding the effect of CMC-544.

Materials and methods

Cells

CD22-positive cell lines used were Epstein–Barr virus (EBV)-positive human lymphoma cell lines, Daudi and Raji, and their mdr-1 DNA-transduced Daudi and Raji sublines, Daudi/MDR and Raji/MDR (Sugimoto *et al*, 1997). $1{\cdot}0 \times 10^7$ and $6{\cdot}3 \times 10^5$ copies of *ABCB1* mRNA (*ABCB1/GAPDH* was 1·261 and 0·078 respectively) were detectable in Daudi/MDR and Raji/MDR respectively, by quantitative polymerase chain reaction (Yajima *et al*, 1998), but it was not detectable in Daudi and Raji cells. Intracellular accumulation of rhodamine-123 (Rh123) shows a large amount of P-gp in Daudi/MDR and Raji/MDR cells (Takeshita *et al*, 2003). After the cells were cultured for 72 h with increasing concentrations of CMC-544, 50% inhibitory concentration values (IC50s) were measured by the dye elusion test with propidium iodide (PI) staining. IC50s of CMC-544 were 7 and 13 ng/ml calicheamicin in Daudi and Raji cells respectively. In contrast, IC50s in Daudi and Raji MDR sublines were 560 and 380 ng/ml respectively. The IC50s of Daudi/MDR and Raji/MDR cells were around 80 and 30 times higher than Daudi and Raji cells respectively. *ABCC1* mRNA and *LRP1* mRNA were not detectable. The CD22-negative cell lines used were a human chronic myeloid leukaemia cell line, K562 (Riken Cell Bank, Tsukuba, Japan); a T-cell leukaemia cell line, Jurkat (Riken Cell Bank); a human acute promyelocytic leukaemia cell line, NB4 (kindly provided by Dr M Lanotte, Hospital Saint-Louis, Paris, France).

These cell lines were cultured in RPMI 1640 medium, supplemented with L-glutamine (2 mmol/l), antibiotics and 10% foetal calf serum (FCS; Gibco BRL, Grand Island, NY, USA), (10% FCS-RPMI) at 37°C. Vincristine sulphate (4 ng/ml) was added every 3 weeks to the culture medium of Daudi/MDR and Raji/MDR cell lines (Sugimoto *et al*, 1997).

After informed consent, peripheral blood cells were collected from five patients with B-CLL, and lymphoma cells were separated from lymph nodes of 14 patients with NHL. The cells were purified by Ficoll–Hypaque centrifugation (Pharmacia, Uppsala, Sweden).

Flow cytometric analyses for CD-phenotype and immunoglobulin on cells

In all analyses, cells were stained by phycoerythrin-cyanin 5.1 (PC5)-conjugated anti-CD45 monoclonal antibody (mAb) (Becton Dickinson Immunocytometry Systems, San Jose, CA, USA) and gated by the pattern of side scatter (SCC) and CD45 expression (CD45-gating) with an Epics XL flow cytometer (Beckman Coulter, Fullerton, CA, USA) (Matsui *et al*, 2002). Cells were additionally stained by fluorescein isothiocyanate (FITC)- or phycoerythrin (PE)-conjugated anti-CD2, CD3, CD4, CD5, CD7, CD8, CD10, CD11c, CD16, CD19, CD20, CD22, CD23, CD25, CD30, CD34, CD56, κ-chain or λ-chain mAbs (Becton Dickinson Immunocytometry Systems) according to the manufacturer's instructions. We examined the ratio of κ- to λ-chain expressing cells in the CD45-gated group and only used samples in which the ratio was 20 times or more.

Specifically, for the detection of CD22, cells were stained with a FITC-labelled anti-CD22 mAb, HIB22 (Becton Dickinson Immunocytometry Systems). Ten thousand events were counted by flow cytometry. The dissociation of mean fluorescence intensity (MFI) of cells that reacted with anti-CD22 mAb and that of the subclass-matched mAb was determined.

In the analysis for internalisation of CMC-544, cells were pre-incubated with CMC-544 (5 ng/ml calichemicin DMH) at 37°C for 1 h, and washed three times. Then the cells were stained with FITC-labelled anti-human IgG mAb (Becton Dickinson Immunocytometry Systems) and incubated with CMC-544-free medium for 2 h. MFI of cells after the incubation was compared to that of before. The ratio (%) of MFI was used as a marker of the internalisation.

Flow cytometric analysis for P-glycoprotein

For P-gp analysis, cells were reacted with biotinylated MRK16 (Fab') mouse mAb or with a subclass-matched control mAb and then stained with streptavidin- FITC (Becton Dikinson Immunocytometry Systems) as previously described (Takeshita *et al*, 2005). The degree of dissociation between the fluorescence intensity of cells that reacted with MRK16 and the respective subclass-matched mAb was analysed by the channel-by-channel subtraction method (Beckman Coulter). The cell count in each channel of the control histogram was subtracted from the cell count in the corresponding channel of the test histogram. The differences for all channels were totalled to calculate P-gp presence (%) (Müller *et al*, 1994; Naito *et al*, 2000; Takeshita *et al*, 2005).

P-gp function was determined by measuring intracellular Rh123 accumulation and its enhancement by MDR modifiers, such as PSC833 (Novartis Pharma, Basel, Swizerland) or MS209 (Mitsui Phamaceuticals, Chiba, Japan), as previously

described (Nakanishi *et al*, 1997; Merlin *et al*, 1998; Matsui *et al*, 2002; Takeshita *et al*, 2005).

Humanized anti-CD22 monoclonal antibody and CMC-544

The humanized IgG_4 anti-CD22 mAb, G5/44, and NAc-γ-calicheamicin DMH-conjugated to the humanized IgG_4 anti-CD22 mAb, CMC-544, were kindly provided by Wyeth Research (Collegeville, PA, USA) (DiJoseph *et al*, 2004). The calicheamicin-conjugated humanized IgG_4 anti-CD33 mAb, GO, and unconjugated NAc-γ-calicheamicin DMH were also provided. After the cells were incubated with various concentrations of CMC-544 or G5/44 at 37°C for 2 h, they were washed and resuspended in 10% FCS-RPMI and prepared for subsequent analysis.

Cell cycle distribution analysis

Cells were incubated with CMC-544 containing 5–100 ng/ml calicheamicin for 2 h and washed. The cell cycle distribution was analysed after incubation in CMC-544-free medium for 72 h. Cells were gently suspended in 1 ml hypotonic fluorochrome solution containing PI. The cell cycle distribution was quantified by flow cytometry (Naito *et al*, 2000; Takeshita *et al*, 2005). These experiments were also analysed in the presence of 50–100 μmol/l Z-VAD-FMK (Calbiochem, Darmstadt, Germany), a caspase inhibitor, to study the apoptotic mechanisms of CMC-544. If samples from patients were contaminated with 5% or more of non-B cells by examining cell-surface antigens described before, malignant cells were sorted by the CD45-gating with a FACS Aria (Becton Dickinson, Franklin Lakes, NJ, USA) prior to cell cycle analysis.

Morphological analysis by a video-microscopic technique

Cells (1×10^5 cells/ml) were plated in a glass-bottomed dish (MatTec Corporation, Ashland, MA, USA) and incubated with CMC-544 containing 10 ng/ml calicheamicin for 2 h before washing. After 24- and 48-h incubations at 37°C in CMC-544 free medium, cells were observed under an inverted Normarski microscope (Axiovert 35; Zeiss, Oberkochen, Germany) as described previously (Naito *et al*, 2000).

Dye exclusion test with PI staining

After incubation of cells with CMC-544 or G5/44 for the indicated periods of time, cells were stained with 0·1 μg/ml PI solution and counted under the microscope (Takeshita *et al*, 2005). Viable cell counts were calculated as follows: (viable cell counts) = (total cell counts) − (PI stained cell counts). The viable cell count following incubation with CMC-544 was compared with that following incubation with G5/44.

The process of CMC-544-induced cell death

Cell death was quantitated using an Apocyto® kit containing Annexin V-Azami-Green and PI (Karasawa *et al*, 2003). Viable cells were not stained by either agent (Annexin−PI−), while early apoptotic cells were stained by Annexin V-Azami-Green (Annexin+PI−), and late apoptotic cells were stained by both agents (Annexin+PI+). Cells damaged via a non-apoptotic mechanism were stained only by PI (Annexin−PI+).

In vitro effect of CMC-544 in the presence of MDR modifiers

Cells were pre-incubated in the presence or absence of 2 μmol/l PSC833 or 5 μmol/l MS209 in a humidified CO_2 incubator at 37°C for 1 h. The cells were then incubated with or without CMC-544 containing 5–100 ng/ml calicheamicin in the presence or absence of 2 μmol/l PSC833 or 5 μmol/l MS209 at 37°C for 2 h. After incubation, the cells were washed three times to remove unbound CMC-544. They were then re-incubated in CMC-544-free medium at 37°C for 24–48 h. The viability of cells just after incubation with CMC-544 was 99·6% by the dye exclusion test, which was carried out as described in our previous reports on GO (Naito *et al*, 2000; Matsui *et al*, 2002; Takeshita *et al*, 2005).

Results

CD22 expression on cell lines

CD22, which was expressed on Daudi and Raji cells, was equally expressed on Daudi/MDR and Raji/MDR cells respectively (Fig 1A). However, it was not expressed on Jurkat, K562 nor NB4 cells. The amount of CD22 was unchanged after a 2-h incubation with the experimental concentration of MDR modifiers, 2 μmol/l PSC833 or 5 μmol/l MS209 (Fig 1A).

Cell growth assay of P-gp negative cells

The viable cell counts of Daudi and Raji cells decreased in a time- and dose-dependent manner at 48 h after incubation with CMC-544 containing 5–100 ng/ml calicheamicin (Fig 1B). However, the change was not observed in CD22 negative Jurkat or NB4 cells.

Cell growth of Daudi/MDR and Raji/MDR in the absence or presence of MDR modifiers, PSC833or MS209

In the absence of PSC833 or MS209, even CMC-544 containing 100 ng/ml calicheamicin did not suppress the cell growth of Daudi/MDR and Raji/MDR cells. In the presence of 2 μmol/l PSC833 or 5 μmol/l MS209, CMC-544 recovered its cytotoxic effect and suppressed the cell growth in a dose-dependent manner (Fig 1C). Cells treated with only PSC833 or MS209 at the same concentrations did not show significant growth changes.

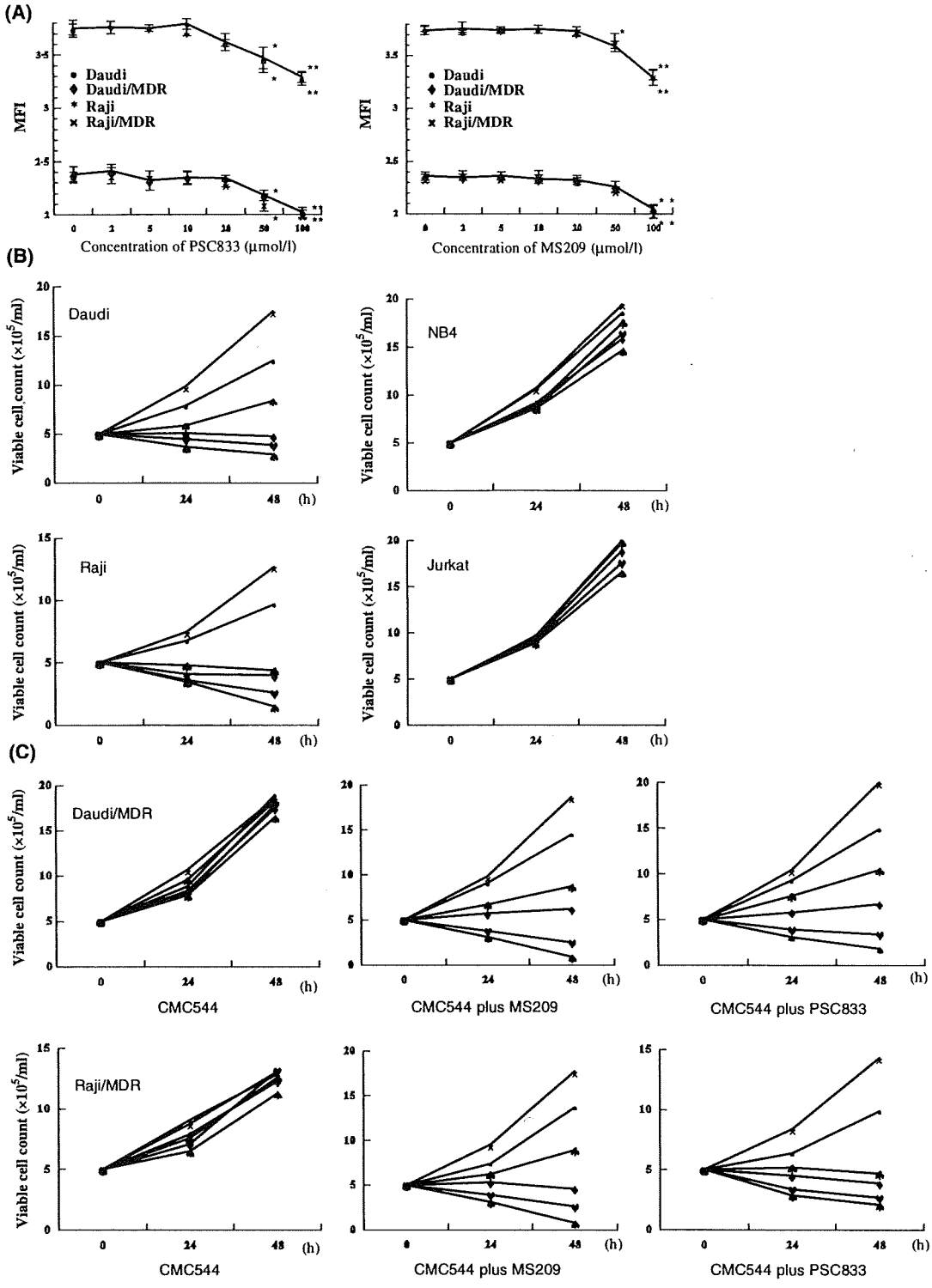

Fig 1. (A) Daudi (●) and Raji (*) cells and their MDR sublines, Daudi/MDR (◆) and Raji/MDR (x), were stained by FITC-labelled anti-CD22 mAb after a 2-h incubation with 0, 2, 5, 10, 20, 50, 100 μmol/l of PSC833 or MS209. CD22 level was not influenced by 0–20 μmol/l of PSC833 or MS209. (B) Cell growth of Daudi, Raji, Jurkat, and NB4 cells analysed by flow cytometry after incubation with G5/44 or various concentrations of CMC-544 for 48 h (x) G5/44, (●) 5 ng/ml, (♣) 10 ng/ml, (◆) 20 ng/ml, (♥) 50 ng/ml and (♠) 100 ng/ml calicheamicin. (C) Cell growth of Daudi/MDR and Raji/MDR cells analysed by flow cytometry at 48 h after incubation with CMC-544 containing 10 ng/ml calicheamicin in the absence or presence of 5 μmol/l MS209 or 2 μmol/l PSC833.

Cell cycle distribution of CD22-positive and negative cells

Cell cycle distribution patterns of Daudi and Raji cells at 0-, 12-, 24-, 48-, 72-h after incubation with CMC-544 containing 5 ng/ml calicheamicin were analysed (Fig 2A). Daudi and Raji cells arrested at the G2/M phase before the hypodiploid portion increased. In the presence of 50–100 μmol/l Z-VAD-fmk, while G2/M arrest was apparent, G0/G1 and G2/M phases were restored thereafter without a following increase in the hypodiploid portion. In Jurkat, NB4 and K562 cells, no effect was observed after the incubation of CMC-544 (data not shown). G5/44 did not affect the cell cycle distribution.

Cell cycle distribution of Daudi/MDR and Raji/MDR sublines

CMC-544 had a dose-dependent effect on the cell cycle distribution of Daudi and Raji cells. The pattern was not changed in either Daudi/MDR or Raji/MDR cells incubated with G5/44 or CMC-544 containing 5–100 ng/ml calicheamicin (Fig 2B). However, in the presence of 2 μmol/l PSC833 (bottom line in Fig 2B) or 5 μmol/l MS209 (data not shown), addition of CMC-544 recovered the effect and arrested the cell cycle in both cell lines at G2/M phase.

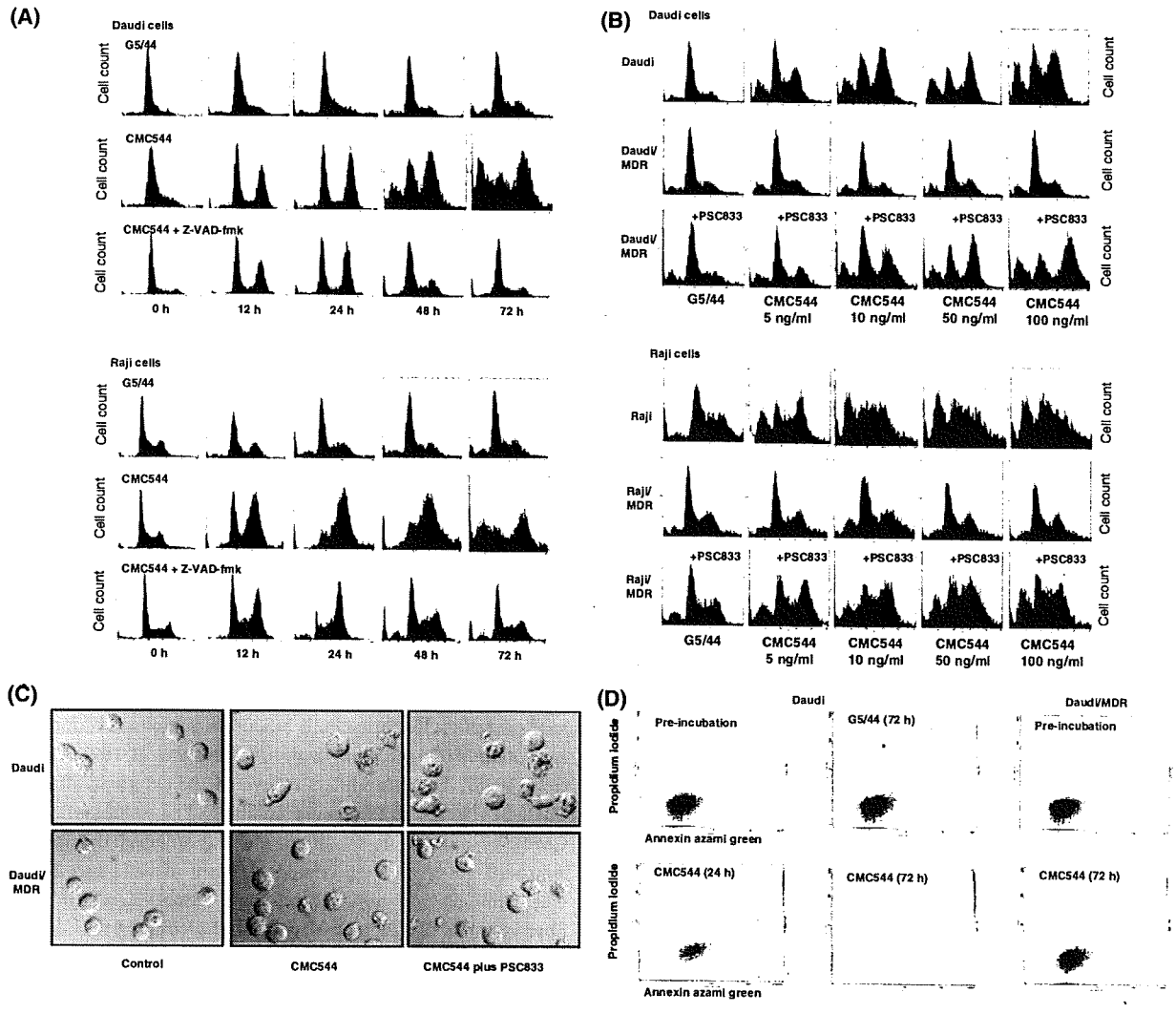

Fig 2. (A) Cell cycle distribution at 0, 12, 24, 48 and 72 h after incubation with G5/44 or CMC-544 with or without 100 μmol/l Z-VAD-fmk. (B) Cell cycle distribution of Daudi and Daudi/MDR cells, and Raji and Raji/MDR cells 48 h after incubation with G5/44 or CMC-544 containing 5, 10, 50 or 100 ng/ml calicheamicin in the absence or presence of 2 μmol/l PSC833. (C) Morphological changes of Daudi and Daudi/MDR cells were observed using a video-microscope. Daudi cells were incubated in medium containing CMC-544 with or without 2 μmol/l PSC833 for 24 h. Original magnification ×400. (D) Apoptotic mechanism of CMC-544 in the figures of Apocyto®. Daudi and Daudi/MDR cells were incubated in medium containing CMC-544 or G5/44, and were stained by PI (vertical lines) and Annexin-V Azami Green (horizontal lines).

Morphological observation by a video-microscopic technique

Daudi cells became enlarged after 24-h incubation with CMC-544 compared with the control cells incubated with G5/44 alone. Morphological changes of apoptosis, characterized by bleb formation and shrinkage of cells, were observed in 35% of the cells (Fig 2C). These morphological changes were rarely observed in the Daudi/MDR cells. CMC-544 recovered the effect in the presence of 2 μmol/l PSC833 (Fig 2C) or 5 μmol/l MS209 (data not shown).

The process of CMC-544-induced cell death

Apoptotic analyses of CMC-544 using an Apocyte® kit are summarized in Fig 2D. After incubation of Daudi cells with CMC-544 containing 10 ng/ml calicheamicin, Annexin−PI− cells decreased concomitantly with an increase of Annexin+PI− and Annexin+PI+ cells in a time dependent manner, while Annexin−PI+ cells did not significantly increase. However, Daudi/MDR cells were not changed significantly at 72 h after the incubation with CMC-544. G5/44 did not change the distributions significantly.

The in vitro cytotoxic effect of CMC-544 in the samples from B-CLL and NHL cases

The relationships among the *in vitro* effect of CMC-544, internalisation, CD22 and P-gp levels were investigated using cells from 19 patients with B-CLL and NHL. The characteristics and results of the cases are summarized in Table I. The *in vitro* effect of CMC-544 was significantly correlated with the amount of CD22 ($P = 0{\cdot}010$), but it was inversely correlated with the amount of P-gp ($P = 0{\cdot}003$) or the percentage increase of intracellular Rh123 level in the presence of PSC833 or MS209 ($P < 0{\cdot}001$) (Fig 3). Additionally, we determined internalisation level of CMC-544 by analysing CMC-544 conjugated fluorescence before and after the incubation of antibody-free medium for 2 h. The damping degree of the fluorescence was not related to cytotoxicity of CMC544, CD22 and P-gp level ($P = 0{\cdot}26$, $P = 0{\cdot}90$ and $P = 0{\cdot}89$ respectively) in the patient samples. Some of the cells that had low sensitivity for CMC544, despite low P-gp levels, had a relatively low CD22 level (Case 14) or low internalisation (Case 4).

Discussion

Antibody-targeted chemotherapy is one of the most promising treatments for refractory or resistant haematological malignancies (Faderl *et al*, 2005; Cheson, 2006; Fanale & Younes, 2007; Taksin *et al*, 2007). For example, calicheamicin-conjugated antibodies have yielded informative results, and GO continues to provide encouraging clinical results. However, drug efflux mediated by P-gp leads to the development of drug resistance to GO, and inhibition of P-gp effectively increases GO-induced cytotoxicity *in vitro* (Naito *et al*, 2000; Matsui *et al*, 2002; Takeshita *et al*, 2005). In fact, P-gp is related to adverse clinical outcomes after GO-based therapy (Walter *et al*, 2007). Our present study suggests that CMC-544, a promising new drug for B-cell malignancies, is also affected by P-gp.

CD22-positive malignant cell lines, such as Daudi and Raji cells, were killed by CMC-544, while CD22-negative cell lines, such as NB4 and Jurkat cells, were not. Similar to GO (Naito *et al*, 2000), CMC-544 arrested the cell cycle at the G2/M phase and increased the hypodiploid portion in Daudi and Raji cells. In the presence of Z-VAD-fmk, while G2/M arrest was apparent, G0/G1 and G2/M phase were restored thereafter without a following increase in hypodiploid portion. The results indicate that the G2/M arrest by CMC544 is transient and a considerable number of cells might undergo apoptosis after release from G2/M arrest caused by the caspase. However, the proportion of cells moving to apoptosis via this pathway is still unclear. The caspase and its inhibitor may have a role in resistance to CMC-544, although they were not examined extensively in this study.

While several studies of CMC-544 have recently been published (DiJoseph *et al*, 2004, 2006, 2007), there is currently no published literature regarding CMC-544 in relation to P-gp. Our study suggested that the effect of CMC-544 may also be affected by P-gp. Using our newly established *MDR1* DNA-transduced Daudi and Raji sublines, we directly investigated the effect of CMC-544 on P-gp, an advantage over previously established drug-resistant cell lines that generally co-express other resistant mechanisms in addition to P-gp. Our results showed that CMC-544 had no effect on the P-gp expressing sublines compared with the parental cell lines, even though the former expressed sufficient levels of CD22. P-gp is a membrane glycoprotein that actively pumps cytotoxic agents out of cells and decreases the intracellular concentration of the agents, independently of their structure (Kartner *et al*, 1985). Therefore, if calicheamicin becomes detached from CMC-544 within the cell, it should be pumped out of the cell by P-gp. This hypothesis was endorsed by a combined use of CMC-544 and MDR modifiers. Both PSC833, a non-immunosuppressive analogue of cyclosporine, and MS209, a quinoline compound, are potent MDR-reversing drugs (Nakanishi *et al*, 1997; Merlin *et al*, 1998). These modifiers recovered the cytotoxic effect of CMC-544 in P-gp expressing sublines. The combination of CMC-544 and MDR modifiers may be an ideal therapeutic approach to treat P-gp-related resistant B-CLL and NHL. Haematologic and non-haematologic toxicities, which were observed in a clinical trial that utilized a combination of GO and MDR modifiers (Tsimberidou *et al*, 2003), might not be worsened in the case of CMC-544 because CD22 is expressed at lower levels in haematopoietic and non-haematopoietic immature cells than CD33 (Tedder *et al*, 1997).

Several resistant mechanisms in the treatment of B-cell malignancies have been reported, including alterations of intracellular cell death pathways, such as p53 and Bcl-2 family

Table I. Characteristics and results of analysed cases.

No	WHO classification	At diagnosis or relapse	Clinical stage	Previous treatment	Prognostic index	Cytotoxicity (%)	CD22 (MFI)	P-gp MRK (%)	P-gp function PSC833 (%)	P-gp function MS209 (%)	Attenuation of fluorescence (%)
1	CLL	Recurrent	Rai (III) Binet(C)	FLU	NA	32	6·4	0·3	0·7	0·5	74
2	CLL	Recurrent	Rai (III) Binet(C)	FLU	NA	15·6	3·6	3·1	2·7	2·5	60
3	CLL	Recurrent	Rai (IV) Binet(C)	FLU, VCR, CPM,	NA	36·9	10·6	0·3	0·1	0	43
4	CLL	Recurrent	Rai (III) Binet(C)	FLU	NA	8·4	3·4	0·1	0	0	18
5	CLL	Diagnosis	Rai (I) Binet(A)	–	NA	32·8	8·9	0·2	0·5	0·3	59
6	DLBCL	Diagnosis	Ia	–	Low intermediate	18·9	1·8	0·6	0·8	0·7	47
7	DLBCL	Diagnosis	IIIa	–	High intermediate	6·3	2·4	7·8	10·3	13·9	41
8	DLBCL	Diagnosis	IA	–	Low intermediate	12·7	5·9	5·6	5·8	4·5	52
9	DLBCL	Diagnosis	Iia	–	Low intermediate	26·6	12·9	1·6	0·9	1·1	35
10	DLBCL	Diagnosis	IIIa	–	Low intermediate	18·9	3·8	0·7	0·5	0·2	41
11	DLBCL	Diagnosis	IIIa	–	High	15·7	4·4	0·9	1·7	2·5	57
12	DLBCL	Diagnosis	IVa	–	High	28·9	5·3	5·7	0·2	0·3	81
13	DLBCL	Relapse	IVa	R-CHOP	High intermediate	4·8	5·7	10·2	14·7	18·2	63
14	DLBCL	Relapse	IIIb	R-CHOP	High intermediate	11·1	1·8	0·7	1·5	1·1	72
15	DLBCL	Relapse	Ivb	R-CHOP	High	6·2	5·5	7·1	12·3	15·7	41
16	FL	Diagnosis	IIIa	–	High	21·0	1·7	1·3	1·1	0·3	17
17	FL	Diagnosis	II	–	Low	35·5	4·9	0·6	0·2	0·1	69
18	FL	Diagnosis	IVa	–	Intermediate	20·5	3·9	1·9	1·4	1·1	61
19	FL	Relapse	IVa	R-CHOP	High	5·6	1	12·3	17·4	9·5	50

WHO, World Health Organisation; CLL, chronic lymphocytic leukaemia; DLBCL, diffuse large B cell lymphoma; FL, follicular lymphoma; FLU, fludarabine; VCR, vincristine; CPM, cyclophosphamide; R, rituximab; CHOP, rituximab, adriamycin, VCR, CPM and predonisolone; MFI, mean fluorescence intensity; NA, not available.

Prognosis was determined according to the International Prognostic Index (IPI) or the Follicular Lymphoma International Prognostic Index (FLIPI).

Amount of P-gp was determined by the fluorescence of reacted MRK16 mAb compared to that of control mAb.

P-gp function was determined by the Rh123 accumulation in the presence or absence of MDR modifiers, PSC833 or MS209.

Attenuation of fluorescence, a marker of internalisation, was measured by the comparison of CMC-544 conjugated fluorescence before and after the incubation with CMC-544-free medium for 2 h. Low percentage indicates low internalisation activity.

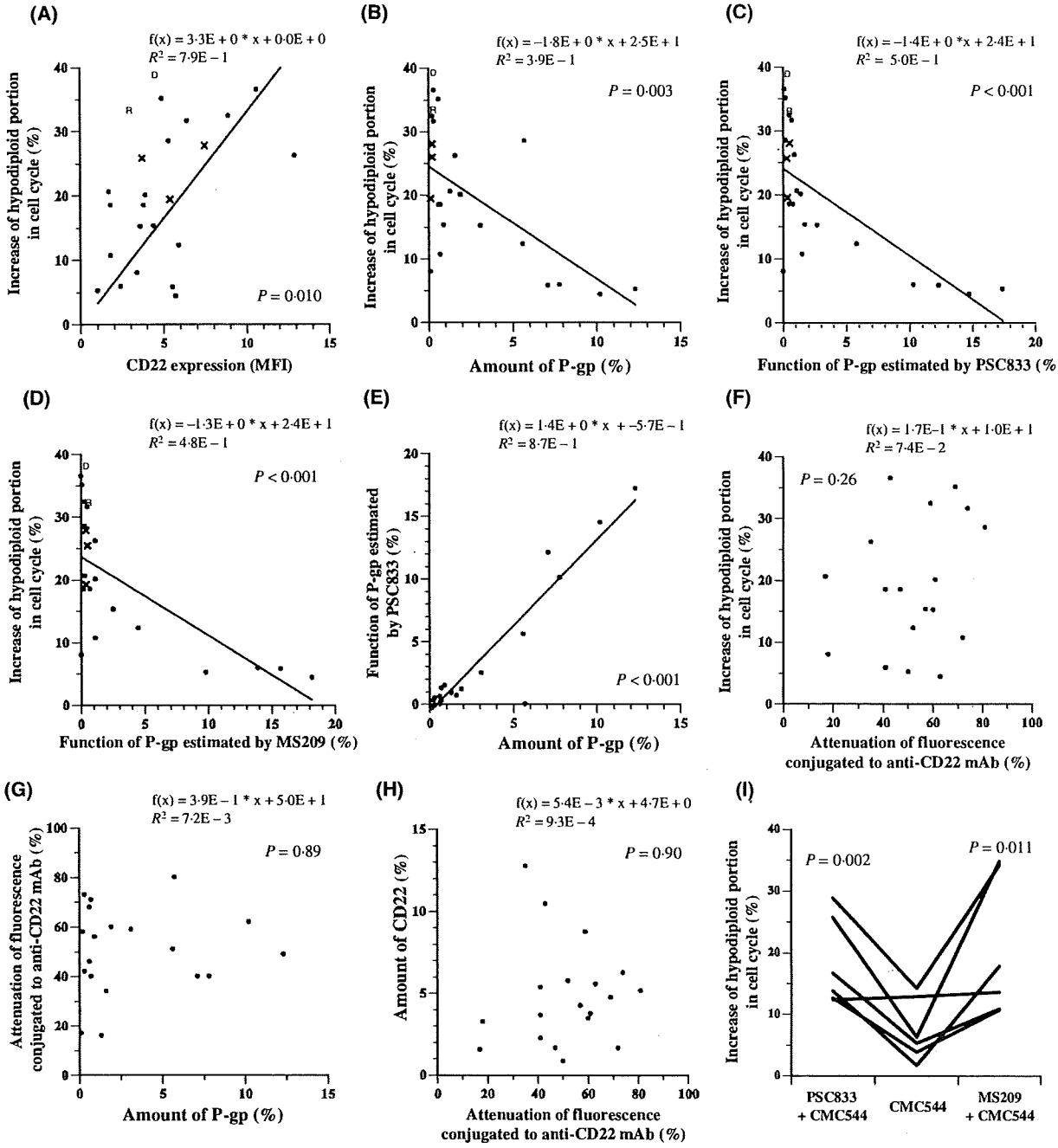

Fig 3. (A) Relationship between the *in vitro* effect of CMC-544 and the CD22 level, (B) the *in vitro* effect of CMC-544 and the amount of P-gp, (C, D) the *in vitro* effect of CMC-544 and the function of P-glycoprotein (P-gp) estimated by Rh123 accumulation with PSC833 (C) or MS209 (D). (F) The relationship between *in vitro* effect of CMC-544 and internalisation. The relationships between these factors were analysed by different combinations (E–H). Each dot represents the data summarized in Table I. The results of normal peripheral B-cells, Daudi and Raji cells were shown as cross dots, D and R respectively. (i) The *in vitro* effect of CMC-544 in the six P-gp positive samples was analysed in the presence of MDR modifiers, PSC833 or MS209, which restored the effect of CMC-544 significantly ($P = 0{\cdot}002$ and $P = 0{\cdot}011$ respectively). (ii) The *in vitro* effect of CMC-544 was determined by the increased hypodiploid portion (%) 72 h after incubation with CMC-544 and compared to that of G5/44.

pathways as well as oxidative stress defence through glutathione peroxidase and ATP-dependent drug efflux pumps (Friedenberg *et al*, 1999; Ohsawa *et al*, 2005; Matthews *et al*, 2006; Montserrat *et al*, 2006; Andreadis *et al*, 2007). The importance of these mechanisms will depend on agents adopted in the treatment. Although P-gp has played a limited role in the drug resistance of B-CLL and NHL, its level is closely related to the intracellular levels of calicheamicin, as

shown in the present study. Therefore, in case of using CMC-544 or other P-gp-dependent drugs, such as doxorubicin and vincristine, it will be important to analyse the level of P-gp and try to overcome its resistant mechanism.

In this study, we also tried to clarify the relationship between P-gp and the effect of CMC-544 using clinical samples from patients with B-CLL and NHL. CMC-544 was less effective on malignant cells from patients with a high amount of P-gp expression. CMC-544 is mostly used for the treatment of refractory or relapsed cases in earlier clinical studies. It should be understood that such patients often express more P-gp. Therefore, CMC-544 treatment alone may have only a limited effect on such patients. In order to achieve maximum effectiveness with this agent, treatments that utilize combination therapy with MDR modifiers or other mAbs may be a promising approach. Moreover, CMC-544 may be more effective when used as a front-line drug for CD22-expressing tumours, before the emergence of P-gp related resistance.

We have also observed the positive relationship between CD22 and the effect of CMC-544 in a study using clinical samples from patients with B-CLL and NHL. While the effect of CMC-544 related to the amount of CD22, the relationship was less prominent than that with P-gp. The cytotoxic effect of CMC-544 in P-gp negative samples varies considerably. Several factors, such as CD22 level, internalisation and other mechanisms might be related to the variation (Goemans *et al*, 2008). In fact, some of the cells that had low sensitivity for CMC-544, despite low P-gp levels, had a relatively low CD22 level or low internalisation. It is difficult to explain the variation in relation to these factors only. Samples from patients in the actual clinical study may clarify this point.

The present study has demonstrated that the effect of CMC-544 depends on the amounts of CD22 and P-gp. Thus, it will be possible to predict the clinical effect of this drug by measuring these parameters. Additionally, *in vitro* analysis of cell cycle effects and observation of apoptotic cells can support the analysis of relevant parameters. Phase I and II studies of CMC-544 are now in progress. This new agent will bring considerable therapeutic benefits to patients with CD22-positive B-CLL and NHL. Possible advantages of concomitant use with an MDR modifier should be discussed in clinical trials. Such an approach might bring an increase in efficacy with or without the worsening of associated adverse events.

Acknowledgements

We express our sincere gratitude to Wyeth Pharmaceuticals Inc. USA for their continuous support and reviewing the manuscript, and to Ms Yoshimi Suzuki, Ms Noriko Anma and Dr Kiyoshi Shibarta (Equipment Centre at Hamamatsu University School of Medicine) for technical assistance. This study was supported by Japanese Grants-in-aid from the Japanese Ministry of Education and Science (Monbukagakusho: 19590552, 17590489).

References

Andreadis, C., Gimotty, P.A., Wahl, P., Hammond, R., Houldsworth, J., Schuster, S.J. & Rebbeck, T.R. (2007) Members of the glutathione and ABC-transporter families are associated with clinical outcome in patients with diffuse large B-cell lymphoma. *Blood*, **109**, 3409–3416.

Auer, R.L., Gribben, J. & Cotter, F.E. (2007) Emerging therapy for chronic lymphocytic leukaemia. *British Journal of Haematology*, **139**, 635–644.

Bonavida, B. (2007) Rituximab-induced inhibition of antiapoptotic cell survival pathways: implications in chemo/immunoresistance, rituximab unresponsiveness, prognostic and novel therapeutic interventions. *Oncogene*, **26**, 3629–3636.

Cheson, B.D. (2006) Monoclonal antibody therapy for B-cell malignancies. *Seminars in Oncology*, **33**, S2–S14.

Coiffier, B. (2007) Rituximab therapy in malignant lymphoma. *Oncogene*, **26**, 3603–3613.

DiJoseph, J.F., Amelino, D.C., Boghhaert, E.R., Khandke, K., Dougher, M.M., Sridharan, L., Kunz, A., Hamann, P.R., Gorovits, B., Udata, C., Moran, J.K., Popplewell, A.G., Stephens, S., Frost, P. & Damle, N.K. (2004) Antibody-tageted chemotherapy with CMC-544: a CD22-tageted imunoconjugate of calicheamicin for the treatment of B-lymphoid malignancies. *Blood*, **103**, 1807–1814.

DiJoseph, J.F., Dougher, M.M., Kalyandrug, L.B., Armellino, D.C., Boghaert, E.R., Hamann, P.R. & Damle, N.K. (2006) Antitumor efficacy of a combination of CMC-544 (inotuzumab ozogamicin), a CD22-targeted cytotoxic immunoconjugate of calicheamicin, and rituximab against non-Hodgkin's B-cell lymphoma. *Clinical Cancer Research*, **12**, 242–249.

DiJoseph, J.F., Dougher, M.M., Armellino, D.C., Evans, D.Y. & Damale, N.K. (2007) Therapeutic potential of CD22-specific antibody-targeted chemotherapy using inotuzumab ozogamicin (CMC-544) for the treatment of acute lymphoblastic leukemia. *Leukemia*, **21**, 2240–2245.

Faderl, S., Coutré, S., Byrd, J.C., Dearden, C., Denes, A., Dyer, M.J., Gregory, S.A., Gribben, J.G., Hillmen, P., Keating, M., Rosen, S., Venugopal, P. & Rai, K. (2005) The evolving role of alemtuzumab in management of patients with CLL. *Leukemia*, **19**, 2147–2152.

Fanale, M.A. & Younes, A. (2007) Monoclonal antibodies in the treatment of non-Hodgkin's lymphoma. *Drugs*, **67**, 333–350.

Friedenberg, W.R., Spencer, S.K., Musser, C., Hogan, T.F., Rodvold, K.A., Rushing, D.A., Mazza, J.J., Tewksbury, D.A. & Marx, J.J. (1999) Multi-drug resistance in chronic lymphocytic leukemia. *Leukemia & Lymphoma*, **34**, 171–178.

Goemans, B.F., Zwaan, C.M., Vijverberg, S.J., Loonen, A.H., Creutzig, U., Hählen, K., Reinhardt, D., Gibson, B.E., Cloos, J. & Kaspers, G.J. (2008) Large interindividual differences in cellular sensitivity to calicheamicin may influence gemtuzumab ozogamicin response in acute myeloid leukemia. *Leukemia*, **22**, 2284–2285.

Hiddemann, W., Buske, C., Dreyling, M., Weigert, O., Lenz, G. & Unterhalt, M. (2006) Current management of follicular lymphomas. *British Journal of Haematology*, **136**, 191–202.

Karasawa, S., Araki, T., Yamamoto-Hino, M. & Miyawaki, A. (2003) A green-emitting fluorescent protein from Galaxeidae coral and its monomeric version for use in fluorescent labeling. *Journal of Biological Chemistry*, **278**, 34167–34171.

Kartner, N., Everrnden-Porelle, D., Bradley, G. & Ling, V. (1985) Detection of P-glycoprotein in multidrug-resistant cell lines by monoclonal antibodies. *Nature*, **316**, 820–823.

Larson, R.A., Sievers, E.L., Stadtmauer, E.A., Löwenberg, B., Estey, E.H., Dombret, H., Theobald, M., Voliotis, D., Bennett, J.M., Richie, M., Leopold, L.H., Berger, M.S., Sherman, M.L., Loken, M.R., van Dongen, J.J., Bernstein, I.D. & Appelbaum, F.R. (2005) Final report of the efficacy and safety of gemtuzumab ozogamicin (Mylotarg) in patients with CD33-positive acute myeloid leukemia in first recurrence. *Cancer*, **104**, 1442–1452.

Matsui, H., Takeshita, A., Naito, K., Shinjo, K., Shigeno, K., Maekawa, M., Yamakawa, Y., Tanimoto, M., Kobayashi, M., Ohnishi, K. & Ohno, R. (2002) Reduced effect of gemtuzumab ozogamicin (CMC-676) on P-glycoprotein and/or CD34-positive leukemia cells and its restoration by multidrug resistance modifiers. *Leukemia*, **16**, 813–819.

Matthews, C., Catherwood, M.A., Larkin, A.M., Clynes, M., Morris, T.C. & Alexander, H.D. (2006) MDR-1, but not MDR-3 gene expression, is associated with unmutated IgVH genes and poor prognosis chromosomal aberrations in chronic lymphocytic leukemia. *Leukemia & lymphoma*, **47**, 2308–2313.

Merlin, J.L., Guerci, A.P., Marchal, S., Bour, C., Colosetti, P., Kataki, A. & Guerci, O. (1998) Influence of SDZ-PSC833 on daunorubicin intracellular accumulation in bone marrow specimens from patients with acute myeloid leukaemia. *British Journal of Haematology*, **103**, 480–487.

Montserrat, E., Moreno, C., Esteve, J., Urbano-Ispizua, A., Giné, E. & Bosch, F. (2006) How I treat refractory CLL. *Blood*, **107**, 1276–1283.

Müller, M.R., Lennartz, K., Nowrousian, M.R., Dux, R., Tsuruo, T., Rajewsky, M.F. & Seeber, S. (1994) Improved flow-cytometric detection of low P-glycoprotein expression in leukaemic blasts by histogram subtraction analysis. *Cytometry*, **15**, 64–72.

Naito, K., Takeshita, A., Shigeno, K., Nakamura, S., Fujisawa, S., Shijo, K., Yoshida, H., Ohnishi, K., Mori, M., Terakawa, S. & Ohno, R. (2000) Caliceamicin-conjugated humanized anti-CD33 monoclonal antibody (gemtuzumab ozogamicin, CMC676) shows cytocydal effect on CD33-positive leukemia cell lines, but is inactive on P-glycoprotein-expressing sublines. *Leukemia*, **14**, 1436–1443.

Nakanishi, O., Baba, M., Saito, A., Yamashita, T., Sato, W., Abe, H., Fukazawa, N., Suzuki, T., Sato, S., Naito, M. & Tsuruo, T. (1997) Potentiation of the antitumor activity by a novel quinoline compound, MS-209, in multidrug-resistant solid tumor cell lines. *Oncology Research*, **9**, 61–69.

Ohsawa, M., Ikura, Y., Fukushima, H., Shirai, N., Sugama, Y., Suekane, T., Hirayama, M., Hino, M. & Ueda, M. (2005) Immunohistochemical expression of multidrug resistance proteins as a predictor of poor response to chemotherapy and prognosis in patients with nodal diffuse large B-cell lymphoma. *Oncology*, **68**, 422–431.

Sugimoto, Y., Sato, S., Tsukahara, S., Suzuki, M., Okochi, E., Gottesman, M.M., Pastan, I. & Tsuruo, T. (1997) Coexpression of a multidrug resistance gene (MDR1) and herpes simplex virus thymidine kinase gene in a bicistronic retroviral vector Ha-MDR-IRES-TK allows selective killing of MDR1-transduced human tumors transplanted in nude mice. *Cancer Gene Therapy*, **4**, 51–58.

Svoboda-Beusan, I., Kusec, R., Bendelja, K., Tudoric-Ghemo, I., Jaksic, B., Pejsa, V., Rabatic, S. & Vitale, B. (2000) The relevance of multidrug resistance-associated P-glycoprotein expression in the treatment response of B-cell chronic lymphocytic leukemia. *Haematologica*, **85**, 1261–1267.

Takeshita, A., Shinjo, K., Naito, K., Matsui, H., Shigeno, K., Nakamura, S., Horii, T., Maekawa, M., Kitamura, K., Naoe, T., Ohnishi, K. & Ohno, R. (2003) P-glycoprotein (P-gp) and multidrug resistance-associated protein 1 (MRP1) are induced by arsenic trioxide (As(2)O(3)), but are not the main mechanism of As(2)O(3)-resistance in acute promyelocytic leukemia cells. *Leukemia*, **17**, 648–650.

Takeshita, A., Shinjo, K., Naito, K., Matsui, H., Sahara, N., Shigeno, K., Horii, T., Shirai, N., Maekawa, M., Ohnishi, K., Naoe, T. & Ohno, R. (2005) Efficacy of gemtuzumab ozogamicin on ATRA- and arsenic-resistant acute promyelocytic leukemia (APL) cells. *Leukemia*, **19**, 1306–1311.

Taksin, A.L., Legrand, O., Raffoux, E., de Revel, T., Thomas, X., Contentin, N., Bouabdallah, R., Pautas, C., Turlure, P., Reman, O., Gardin, C., Varet, B., de Botton, S., Pousset, F., Farhat, H., Chevret, S., Dombret, H. & Castaigne, S. (2007) High efficacy and safety profile of fractionated doses of Mylotarg as induction therapy in patients with relapsed acute myeloblastic leukemia: a prospective study of the alfa group. *Leukemia*, **21**, 66–71.

Tedder, T.F., Tuscano, J., Sato, S. & Kehrl, J.H. (1997) CD22, a B lymphocyte-specific adhesion molecule that regurates antigen receptor signaling. *Annual Review of Immunology*, **15**, 481–504.

Tsimberidou, A., Estey, E., Cortes, J., Thomas, D., Faderl, S., Verstovsek, S., Garcia-Manero, G., Keating, M., Albitar, M., O'Brien, S., Kantarjian, H. & Giles, F. (2003) Gemtuzumab, fludarabine, cytarabine, and cyclosporine in patients with newly diagnosed acute myelogenous leukemia or high-risk myelodysplastic syndromes. *Cancer*, **97**, 1481–1487.

Walter, R.B., Gooley, T.A., van der Velden, V.H., Loken, M.R., van Dongen, J.J., Flowers, D.A., Bernstein, I.D. & Appelbaum, F.R. (2007) CD33 expression and P-glycoprotein-mediated drug efflux inversely correlate and predict clinical outcome in patients with acute myeloid leukemia treated with gemtuzumab ozogamicin monotherapy. *Blood*, **109**, 4168–4170.

Yajima, T., Yagihashi, A., Kameshima, H., Kobayashi, D., Furuya, D., Hirata, K. & Watanabe, N. (1998) Quantitative reverse transcription-PCR assay of the RNA component of human telomerase using the *Taq*Man fluorogenic detection system. *Clinical Chemistry*, **44**, 2441–2445.

Zein, N., Sinha, A.M., McGahren, W.J. & Ellestad, G.A. (1988) Calicheamicin gamma 1I: an antitumor antibiotic that cleaves double-stranded DNA site specifically. *Science*, **240**, 1198–1201.

Leukemia (2009) 23, 1329–1336

www.nature.com/leu

ORIGINAL ARTICLE

CMC-544 (inotuzumab ozogamicin), an anti-CD22 immuno-conjugate of calicheamicin, alters the levels of target molecules of malignant B-cells

A Takeshita[1,2], N Yamakage[1], K Shinjo[2], T Ono[2], I Hirano[2], S Nakamura[2], K Shigeno[2], T Tobita[3], M Maekawa[1], H Kiyoi[4], T Naoe[5], K Ohnishi[2], Y Sugimoto[6] and R Ohno[7]

[1]Department of Laboratory Medicine, Hamamatsu University School of Medicine, Higashi-ku, Hamamatsu, Japan; [2]Department of Internal Medicine, Hamamatsu University School of Medicine, Higashi-ku, Hamamatsu, Japan; [3]Department of Hematology, Yaizu City Hospital, Yaizu, Japan; [4]Department of Infectious Diseases, Nagoya University, Chikusa-ku, Nagoya, Japan; [5]Department of Hematology and Oncology, Nagoya University, Chikusa-ku, Nagoya, Japan; [6]Graduate School of Pharmaceutical Sciences, Keio University, Minato-ku, Tokyo, Japan and [7]Aichi Cancer Center, Chikusa-ku, Nagoya, Japan

We studied the effect of CMC-544, the calicheamicin-conjugated anti-CD22 monoclonal antibody, used alone and in combination with rituximab, analyzing the quantitative alteration of target molecules, that is, CD20, CD22, CD55 and CD59, in Daudi and Raji cells as well as in cells obtained from patients with B-cell malignancies (BCM). Antibody inducing direct antiproliferative and apoptotic effect, complement-dependent cytotoxicity (CDC) and antibody-dependent cellular cytotoxicity (ADCC) were tested separately. In Daudi and Raji cells, the CDC effect of rituximab significantly increased within 12 h following incubation with CMC-544. The levels of CD22 and CD55 were significantly reduced ($P<0.001$ in both cells) after incubation with CMC-544, but CD20 level remained constant or increased for 12 h. Similar results were obtained in cells from 12 patients with BCM. The antiproliferative and apoptotic effect of CMC-544 were greater than that of rituximab. The ADCC of rituximab was not enhanced by CMC-544. Thus, the combination of CMC-544 and rituximab increased the *in vitro* cytotoxic effect in BCM cells, and sequential administration for 12 h proceeded by CMC-544 was more effective. The reduction of CD55 and the preservation of CD20 after incubation with CMC-544 support the rationale for the combined use of CMC-544 and rituximab.
Leukemia (2009) **23**, 1329–1336; doi:10.1038/leu.2009.77;
published online 16 April 2009
Keywords: CMC-544; chronic lymphoid leukemia (CLL); malignant lymphoma; monoclonal antibody; rituximab

Introduction

Rituximab, a chimeric monoclonal antibody (mAb) that binds to CD20, has greatly improved therapy for B-cell malignancies (BCM) including non-Hodgkin's lymphoma and chronic lymphoblastic leukemia.[1–4] Nevertheless, a considerable percentage of patients are refractory to treatment with rituximab and relapse after an initial response. Several resistant mechanisms have been proposed including escape into CD20-negative cells by limited surface antigen renewal, cell membrane drug efflux pumps, escape into the resting phase of the cell cycle, enhancement of complement inhibitory factors, alterations in intracellular signaling or cell death pathways, FcγRIIIA polymorphism and reduction of effector cells.[5] Above all, downregulation of CD20 and enhancement of complement inhibitory factors plays an important role in acquired resistance to rituximab. Investigation of complement inhibitory factors demonstrated that CD55 plays an important role as a regulator of complement-dependent cytotoxicity (CDC) in malignant B-cells, and that its expression correlated with resistance to CDC,[6,7] which is one of the main mechanisms of action in the treatment of rituximab.

To overcome resistance to rituximab, several new agents have been developed, including radioimmunotherapy and mAbs against targets other than CD20.[2,8,9] Among them, CMC-544 has been introduced as a promising agent to treat refractory/resistant BCM. CMC-544 is a conjugate of *N*-acetyl γ-calicheamicin dimethyl hydrazide (NAc γ-calicheamicin DMH) and a recombinant humanized antibody (IgG_4) directed against the CD22 antigen.[10] Calicheamicin, a very potent antitumor antibiotic agent, binds to the minor groove of DNA in a sequence-specific manner and breaks double-stranded DNA.[11] Preliminary data from ongoing clinical trials reveal that CMC-544 is efficacious against recurrent/refractory B-cell lymphomas with manageable thrombocytopenia reported as the most significant toxicity.[12]

Concomitant use of CMC-544 and rituximab is an ideal therapeutic method because these agents have a different target molecule and mechanism of action. In fact, the additive combination efficacy of CMC-544 and rituximab was shown against xenogenic BCM in severe combined immunodeficient mice.[13] However, the mechanism of the combination efficacy and the best administration schedule have not yet been elucidated. In this study, we attempted to clarify them from the viewpoint of the alteration of target molecules, that is, CD20, CD22, CD55 and CD59, which are essential for the action of these mAbs.

Materials and methods

Cells

CD22-positive cell lines used were: human lymphoma cell lines, Daudi and Raji, and their mdr-1 DNA-transduced sublines, Daudi/MDR and Raji/MDR.[14] Daudi/MDR and Raji/MDR had detectable mdr-1 messenger RNA (mRNA) and P-glycoprotein. The CD22-negative cell lines used were K562 (Riken Cell Bank, Tsukuba, Japan), Jurkat (Riken Cell Bank) and NB4 (kindly provided by Dr M Lanotte, Hospital Saint-Louis, Paris, France). These cell lines were cultured in RPMI-1640 supplemented with L-glutamine (2 mM), antibiotics and 10% fetal calf serum (FCS) (Gibco BRL, Grand Island, NY, USA) (10% FCS-RPMI) at 37 °C in a humidified 5% CO_2 incubator.

Correspondence: Professor A Takeshita, Laboratory and Internal Medicine, Hamamatsu University School of Medicine, 1-20-1 Handayama, Higashiku, Hamamatsu, Shizuoka 431-3192, Japan.
E-mail: akihirot@hama-med.ac.jp
Received 20 August 2008; revised 4 March 2009; accepted 12 March 2009; published online 16 April 2009

After informed consent, malignant cells were obtained from 12 patients with BCM. Lymphocytes were collected from the peripheral blood of eight patients with chronic lymphoblastic leukemia. Lymphoma cells were separated from the lymph nodes of four patients with large B-cell non-Hodgkin's lymphoma, and purified by density gradient with Ficoll-Paque (Pharmacia, Uppsala, Sweden).

Flow cytometry for CD20, CD22, CD55 and CD59

For the detection of CD20, CD22, CD45, CD55 and CD59, cells were stained with fluorescein isothiocyanate (FITC) or phycoerythrin (PE)-conjugated anti-CD20, anti-CD22, anti-CD55 or anti-CD59 mAbs in addition to Cy7-conjugated anti-CD45 mAb (Becton Dickinson Immunocytometry Systems, San Jose, CA, USA), according to the manufacturer's instructions.[15] Ten thousand events were counted and mean fluorescence intensities (MFIs) were calculated using an Epics XL flow cytometer (Beckman Coulter, Fullerton, CA, USA). All measurements were performed in triplicate.

Real-time reverse-transcription polymerase chain reaction (RT-PCR) assay for CD20, CD22, CD55, CD59 and GAPDH mRNA in Daudi and Raji cells

The levels of CD20, CD22, CD55, CD59 and GAPDH mRNA in Daudi or Raji cells were measured by real-time RT-PCR. In brief, total cellular RNA was isolated using an RNeasy Plus Mini kit (Qiagen, Tokyo, Japan). The extracted RNA was reverse transcribed by random primers and Super Script III reverse transcriptase (Invitrogen Japan, Tokyo, Japan). Complementary DNA (cDNA) fragments were amplified by PCR using designed specific primers: forward (5′-CTCTCTGGGGAGGCATTATGTA-3′) and reverse (5′-GTAACAGTATTGGGTAGATGGGGAG-3′) for CD20; forward (5′-CAGAATACATTCACGCTAAACCTG-3′) and reverse (5′-AACACTGGGGTTACTGGAATTGTA-3′) for CD22; forward (5′-TTCAGGCAGCTCTGTCCAGTG-3′) and reverse (5′-GAGGCTGAAGTGGAAGGATCG-3′) for CD55; forward (5′-CTGTGGACAATCACAATGGGAATGGGA-3′) and reverse (5′-GGTGTTGACTTAGGGATGAAG-3′) for CD59; and forward (5′-AAGGTCATCCCAGAGCTGAA-3′) and reverse (5′-ATGTCA TCATACTTGGCAGGTT-3′) for GAPDH using Power SYBR Green PCR Master Mix kit (Takara Bio Inc., Kusatsu, Japan) with an automatic 7500 Fast Real-Time PCR System (Applied Biosystems, Tokyo, Japan).[16–18] The data were expressed on a log scale as the relative expression to GAPDH. All measurements were performed in triplicate.

Monoclonal antibodies and NAC-calicheamicin DMH

Humanized IgG_4 anti-CD22 mAb (G5/44) and NAc-γ-calicheamicin DMH conjugated one (CMC-544) as well as calicheamicin-conjugated humanized IgG_4 anti-CD33 mAb (GO) and unconjugated NAc-γ-calicheamicin DMH were kindly provided by Wyeth Research (Collegeville, PA, USA). Rituximab was purchased from Zenyaku Co. (Tokyo, Japan).

Cell cycle distribution analysis

Cells suspended in 1 ml hypotonic fluorochrome solution containing propidium iodide (PI) (Sigma, St Louis, MO, USA) were analyzed by flow cytometry as described earlier[15,19] after incubation with CMC-544 containing 1–100 ng/ml calichemicin DMH for 72 h.

Morphological analysis by video-microscopic technique

Cells were plated in a glass-bottomed dish (MatTec Corporation, Ashland, MA, USA) at a concentration of 10^5 cells per ml in a medium containing CMC-544 (10 ng/ml calichemicin DMH) or an equivalent amount of G5/44. After 12 and 24 h incubations at 37 °C, cells were observed under an inverted Normarski microscope (Axiovert 35; Zeiss, Oberkochen, Germany) as described previously.[19]

Laser microscopy

Cells were incubated with CMC-544 or G5/44 for 12–24 h at 37 °C before staining with fluorescence-labeled mAbs (described in *Flow cytometry for CD20, CD22, CD55 and CD59*). Cells were placed on a non-fluorescent glass slide and observed by the C1si real spectral imaging system (Nikon Instech, Kawasaki, Japan). The fluorescence of FITC and phycoerythrin were detected simultaneously.

Dye exclusion test with propidium iodide (PI) staining

After the incubation of cells with CMC-544, G5/44 or rituximab for the indicated periods of time, cells were stained with 0.1 μg/ml PI solution and counted under the microscope.[20] Viable cell counts were calculated as follows: (viable cell count) = (total cell count)−(PI-stained cell count).

Direct antiproliferative and apoptotic effect of CMC-544

Three possible mechanisms responsible for the combined effect of CMC-544 and rituximab were investigated separately: direct antiproliferative and apoptotic effects of the mAb, CDC and antibody-dependent cellular cytotoxicity (ADCC). These assays were conducted after the incubation of Daudi and Raji cells with CMC-544 either in the presence or absence of rituximab.

The antiproliferative effect of rituximab in the presence and absence of CMC-544 or G5/44 was determined by a viable cell count in triplicate. The apoptotic effect was analyzed by cell cycle distribution. In brief, 10^6 per ml viable cells were incubated in the presence or absence of CMC-544 containing 1–10 ng/ml calichemicin DMH for 2 h, washed three times and then incubated with or without 20 μg/ml rituximab for 72 h. Separately, all of the cells were incubated in the presence of 10 μl per 10^6 cells of anti-human IgG goat antibody $F(ab)_2$ (Becton Dickinson Immunocytometry Systems) to enhance the cross-linking effect of rituximab on the cell surface.

Complement-dependent cytotoxicity

The CDC effect was measured by a dye exclusion test in triplicate. After 10^6 per ml cells were incubated with or without rituximab in the presence of fresh human AB serum for 2 h at 37 °C, cells were placed on ice to stop the CDC reaction. Viable cells were counted immediately after incubation and compared with those counted before incubation.[21]

The enhancement of the CDC effect was studied in a similar way in the presence of CMC-544 or G5/44. Specifically, after cells were incubated with or without CMC-544 (5 ng/ml calichemicin DMH) or G5/44 at 37 °C for 2 h, they were washed three times to remove unbound antibodies. The viability of cells before incubation with CMC-544 was 99.8%. After the cells were re-incubated in CMC-544- and rituximab-free medium at 37 °C for 0–48 h, CDC was analyzed as described above.

After the first 30 min of the CDC assay, a part of the cells was placed on ice to stop the reaction, and analyzed the compliment deposition on the cells. This was determined by flow cytometry

after staining with FITC-anti-human C3c rabbit antibody (Dako, Glostrup, Denmark) according to the manufacturer's instructions. MFIs were compared among the groups.

Antibody-dependent cellular cytotoxicity assays

Total mononuclear cells were obtained by Ficoll-Paque centrifugation and natural killer cells were enriched to 78–91% by an Easy Sep human positive natural killer cell kit (Invitrogen). Concurrently, 10^6 per ml target cells were stained with PKH67 using a MINI67 cell linker kit (Sigma).[22] After the PKH67-stained target cells ($PKH67^+$) were incubated in the presence or absence of CMC-544 containing 5 ng/ml calichemicin DMH or equivalent amount of G5/44 for two hours and washed three times, they were co-cultured with 10^4 per ml natural killer cells in triplicate with or without 2 μg/ml rituximab for 4 h at 37 °C. Then the cells were stained with 0.1 μg/ml PI solution and analyzed by flow cytometry. Target cells damaged by ADCC were classified as $PKH67^+PI^+$ cells, whereas viable target cells were classified as $PKH67^+PI^-$ cells.

Statistical analyses

The data of real-time PCR and CDC, shown as means ± s.d., were analyzed and compared using the Student's *t*-test. MFIs from flow cytometry were analyzed by paired *t*-test.

Results

CD20, CD22, CD55 and CD59 expression on cells before and after incubation with CMC-544 as analyzed by flow cytometry

CD20 and CD22 were expressed on more than 99% of Daudi and Raji cells. CD55 was expressed on 72 and 57% of these cells, respectively. They were similarly expressed on Daudi/MDR and Raji/MDR cells (71 and 59%, respectively). However, CD20 and CD22 were not expressed on Jurkat, K562 or NB4 cells (data not shown).

To assess the effect of CMC-544 on antigen expression, cells were cultured for 2 h in a medium containing CMC-544 or G5/44, switched to an antibody-free medium and then examined at various time points thereafter to determine the levels of CD20, CD22, CD55 and CD59 on the cells. After 12–24 h, the level of CD22 on CMC-544-treated cells had decreased relative to that on G5/44-treated cells (Figure 1a) and continued to decrease, with the reduction of cell viability determined by PI staining (83 and 47% at 48 and 72 h, respectively in Daudi cells), and with apoptotic morphological changes determined by microscopic observation (38 and 64% at 48 and 72 h, respectively in Daudi cells). In contrast, the level of CD20 remained constant or increased after 24 h (Figure 1a), but decreased at 48 h (data not shown). Thereafter the level of CD55 significantly decreased after 12–24 h, and continued to decrease further. However, the level of CD59 did not change significantly. The levels of CD20, CD22, CD55 and CD59 on Daudi/MDR and Raji/MDR cells did not change after incubation with CMC-544 (data not shown). Further, the levels of these antigens did not change after incubation with G5/44 or GO (data not shown).

CD20, CD22 and CD55 expression on cells before and after incubation with CMC-544 as analyzed by laser microscopy

The levels of CD20, CD22 and CD55 on Daudi cells were also analyzed by laser microscopy. The levels of antigens before and after exposure to CMC-544 or G5/44 were compared (Figure 2a). Although the level of CD20 did not change significantly, that of CD22 and CD55 significantly decreased after 24 h when compared with the controls. These results are compatible with the data analyzed by flow cytometry. Similar results were obtained in Raji cells (data not shown).

CD20, CD22, CD55 and CD59 expression on cells before and after incubation with CMC-544 as analyzed by real-time RT-PCR

After incubating in a medium containing CMC-544 or G5/44 for 2 h, cells were cultured in an antibody-free medium and harvested at 1-, 3-, 6- and 12-h time points. The levels of CD20, CD22, CD55 and CD59 mRNA in Daudi or Raji cells were measured by real-time RT-PCR and normalized to GAPDH mRNA level (Figure 2b). The levels of CD22 and CD55 mRNA in CMC-544-treated cells began to decrease at 6-h and was significantly lower at 12-h. On the other hand, the levels of CD20 and CD59 mRNA did not change significantly. These changes observed in Daudi and Raji cells were not in Daudi/MDR and Raji/MDR cells. G5/44 had no effect on these mRNA levels.

CD20, CD22, CD55 and CD59 expression on patients' samples of BCM before and after incubation with CMC-544 as analyzed by flow cytometry

Quantitative alterations of CD20, CD22, CD55 and CD59 levels were also analyzed in samples from 12 patients with BCM. The level of CD22 decreased after incubation with CMC-544 in the samples from all patients ($P<0.001$). The level of CD20 was constant in the samples from four patients but increased in eight patients. Although the level of CD55 decreased significantly ($P<0.001$), that of CD59 did not decrease ($P=0.096$). Results derived from four representative samples are shown in Figure 1b. Cell sizes increased in all samples after 24 h incubation as determined by a two-dimensional analyses of forward and side scatter (Figure 3a). The enlargement was confirmed by morphological changes observed by microscopy (Figure 3b).

Direct antiproliferative and apoptotic effects of rituximab in combination with CMC-544

The antiproliferative effect was determined by a viable cell count after incubation with either rituximab, CMC-544 or both agents (Figure 4a). Viable cell counts after incubation with rituximab, CMC-544 or both agents compared with those before the incubation were 93, 45 and 41% in Daudi cells, and 96, 37 and 34% in Raji cells, respectively.

The apoptotic effect was investigated by cell cycle after incubation with either rituximab, CMC-544 or both agents (Figure 4a). The hypodiploid portion after incubation with rituximab, CMC-544 or both agents increased 4, 35 and 38% in Daudi cells, 8, 56 and 60% in Raji cells, respectively.

Thus, the antiproliferative and apoptotic effects of rituximab alone were significantly less than that of CMC-544 alone. The same results were obtained in BCM cells. The antiproliferative and apoptotic effects were not observed in incubation with G5/44 (data not shown).

Combination effect of CMC-544 on CDC caused by rituximab

The viable cell count significantly decreased after incubation with rituximab through CDC in Daudi and Raji cells. However,

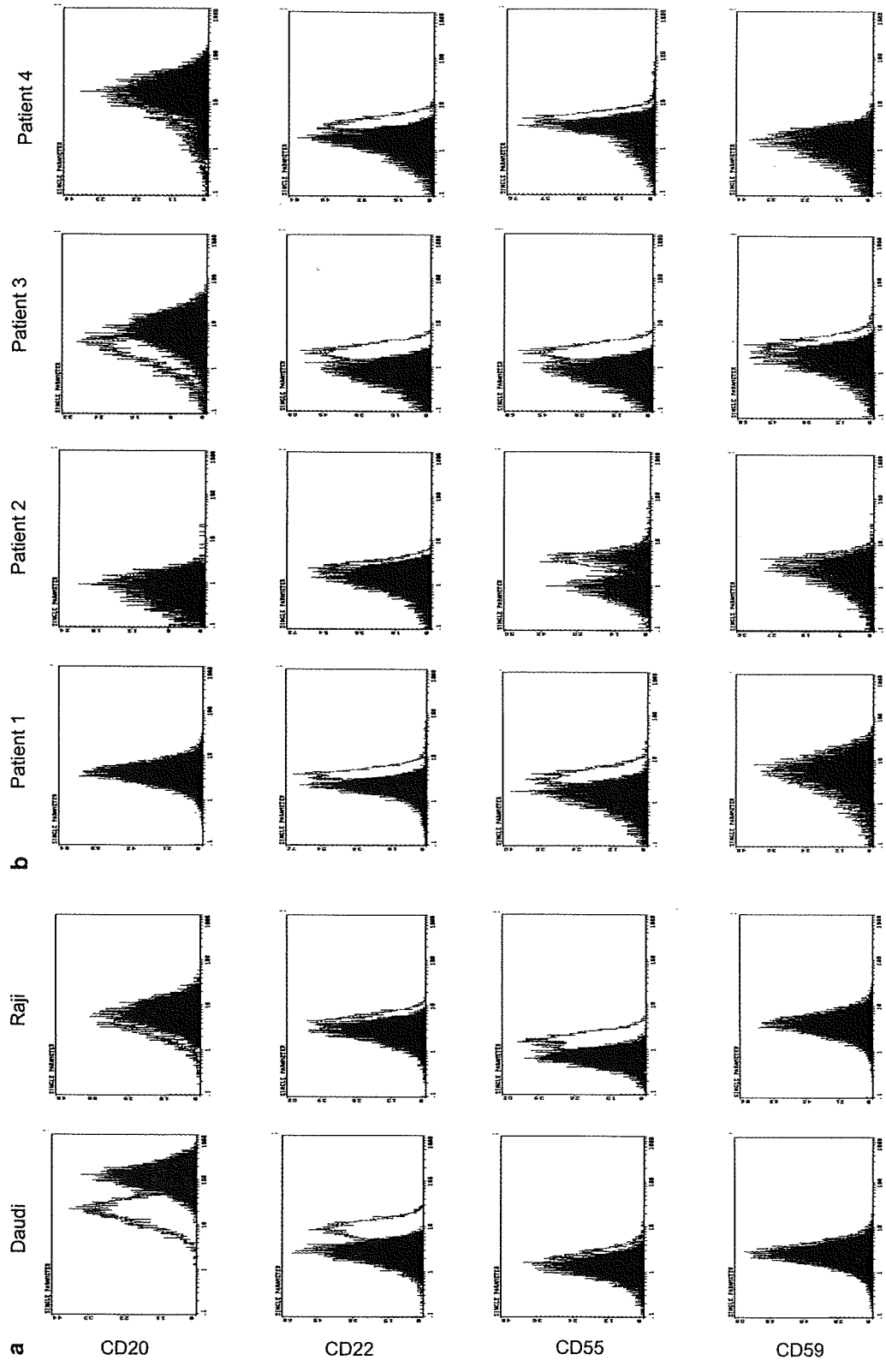

Figure 1 (**a**) The levels of CD20, CD22, CD55 and CD59 antigens on Daudi and Raji cells were analyzed by flow cytometry after exposure to a medium with or without CMC-544. The horizontal lines show the fluorescence intensity, and the vertical lines show the levels of CD20, CD22, CD55 or CD59. White and black histograms show the data obtained after cells were incubated with G5/44 or CMC-544, respectively. The levels of CD22 and CD55 decreased 12–24 h after CMC-544 exposure, whereas those of CD20 increased. The levels of CD59 did not change significantly. (**b**) Results are shown from four representative patients with BCM that contained a sufficient number of cells for analysis. The same results were obtained for the remaining samples.

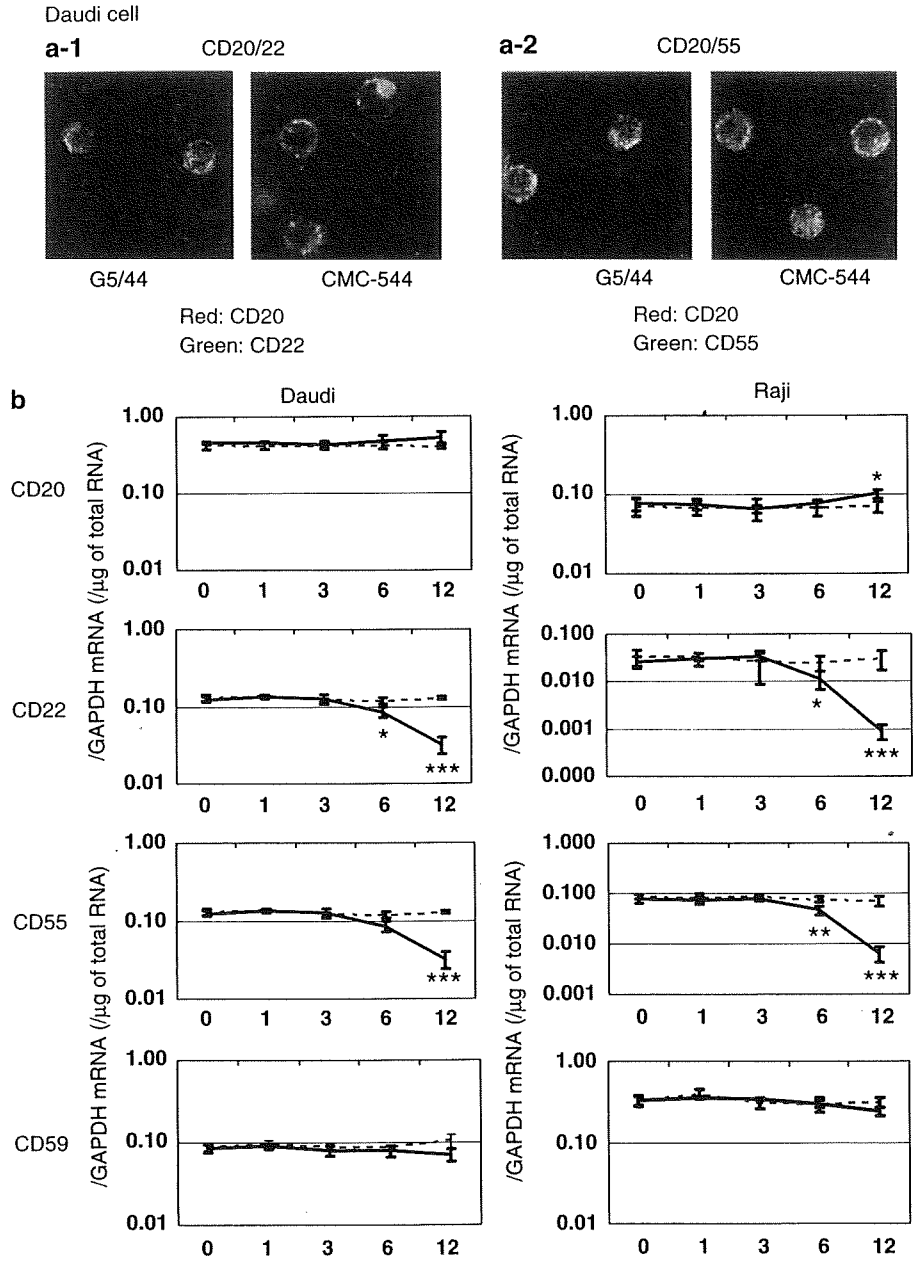

Figure 2 (**a**) Laser scanning microscope images taken 24 h after a 2 h incubation in a medium containing CMC-544 or G5/44. (**a-1**) Daudi cells were stained with PE-conjugated anti-CD20 mAb (red) and FITC-conjugated anti-CD22 mAb (green). (**a-2**) Daudi cells stained by PE-conjugated anti-CD20 mAb (red) and FITC-conjugated anti-CD55 mAb (green). The levels of CD22 and CD55 were significantly reduced, whereas the CD20 expression was constant or increased. (**b**) The levels of CD20, CD22, CD55 and CD59 mRNA in Daudi and Raji cells were analyzed by real-time RT-PCR. After incubating in a medium containing CMC-544 (straight lines) or G5/44 (dotted lines) for 2 h, cells were cultured in an antibody-free medium and harvested at 1-, 3-, 6- and 12-h time points for real-time RT-PCR. The levels of CD22 and CD55 mRNA were significantly reduced after CMC-544 exposure, whereas those of CD20 and CD59 mRNA were maintained. The quantitative data were expressed on a log scale as the relative expression to GAPDH. The data after incubation with CMC-544 were compared with that of G5/44. $^{*}P<0.05$, $^{**}P<0.01$ and $^{***}P<0.001$.

no effect on CDC was observed with CMC-544 or G5/44 alone (Figure 4b). Furthermore, the CDC caused by rituximab was not enhanced by simultaneous incubation with CMC-544 or G5/44.

To determine if CDC is enhanced by the sequential incubation of rituximab and CMC-544, Daudi and Raji cells were first incubated in a medium containing CMC-544 for 2 h, incubated for 12 h in an antibody-free medium, and then CDC by rituximab was analyzed. The CDC effect of rituximab was significantly increased 12 h after incubation with CMC-544 ($P<0.001$) (Figure 4b). G5/44 did not increase the CDC effect of rituximab. Similar results were obtained from patients' samples (Figure 4c).

After the first 30 min of the CDC assay using rituximab and AB serum, compliment deposition on the cells was analyzed by flow cytometer. The level of C3 on CMC-544-treated cells increased to G5/44-treated cells significantly ($P=0.034$) (Figure 4d).

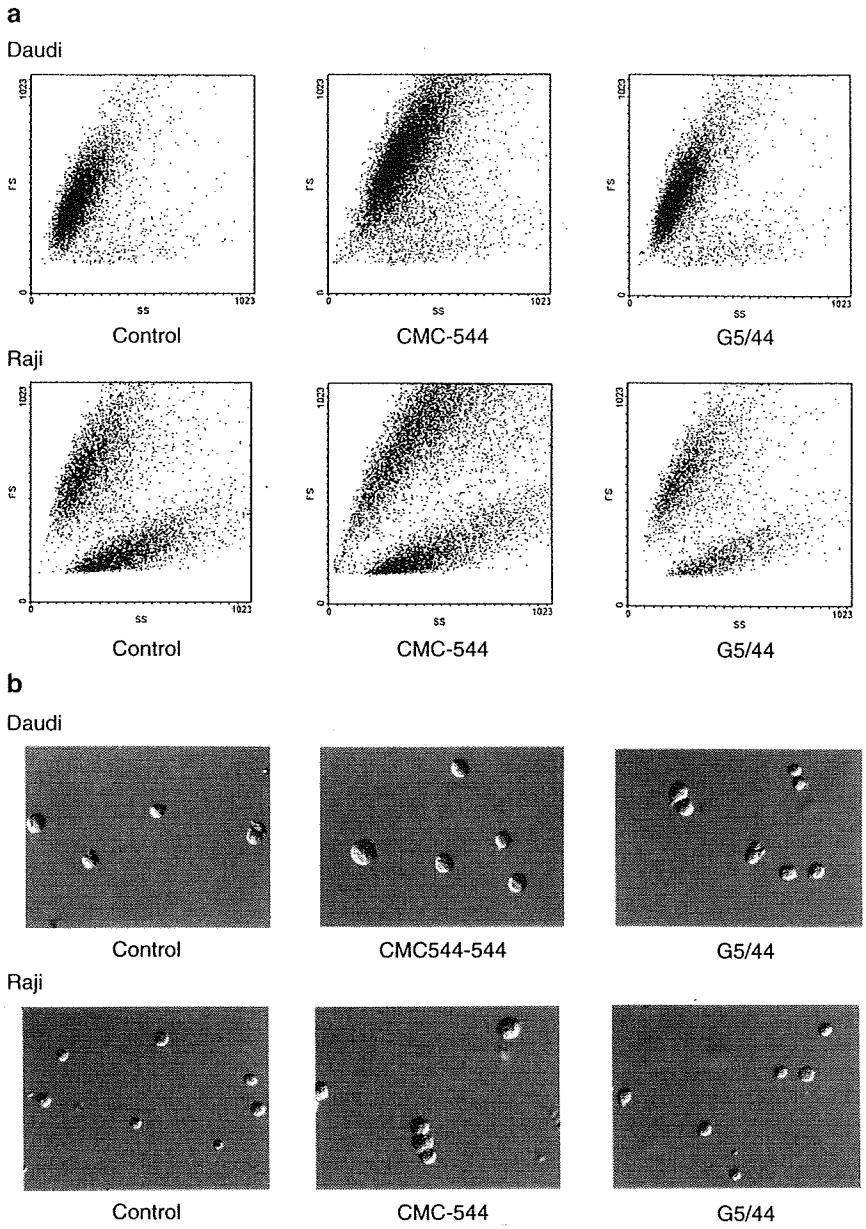

Figure 3 (**a**) Forward scatter (FS) and side scatter analyzed by flow cytometry 24 h after exposure of Daudi and Raji cells to medium with or without CMC-544. Fluorescence intensity of FS increased after exposure to CMC-544 compared with controls. (**b**) Morphological changes of Daudi and Raji cells 24 h after exposure to CMC-544 or G5/44. Cells were enlarged 12–24 h after incubation with CMC-544.

Combination effect of CMC-544 on ADDC caused by rituximab

We counted viable target cells, that is, $PKH67^+PI^-$ cells, and compared them before and after incubation with rituximab or CMC-544 in Daudi and Raji cells. Forty-nine percent of $PKH67^+PI^-$ cells changed to $PKH67^+PI^+$ after a 4 h incubation with rituximab, whereas 9 and 2% changed after incubation with CMC-544 or G5/44, respectively. The change was not significant for simultaneous incubation with rituximab and CMC-544 (53%) or G5/44 (51%) ($P=0.11$ and $P=0.21$, respectively) nor was it increased by sequential incubation with rituximab and CMC-544. Similar results were obtained from the patients' samples (data not shown).

Discussion

Rituximab has provided many encouraging clinical outcomes in the treatment of BCM.[23] CMC-544, recently introduced, is also a promising agent for BCM. These mAbs target different antigens and have different antitumor mechanisms. We investigated the effects of these agents from the viewpoint of alteration of the target molecules, that is, CD20, CD22, CD55 and CD59, which are essential for their action, and attempted to clarify the rationale for the advantage in combination of rituximab and CMC-544.

CD20 is a good target for BCM because it is expressed at high levels and is not downregulated after antibody binding.[2] Although malignant B-cells are heterogeneous and multi-step

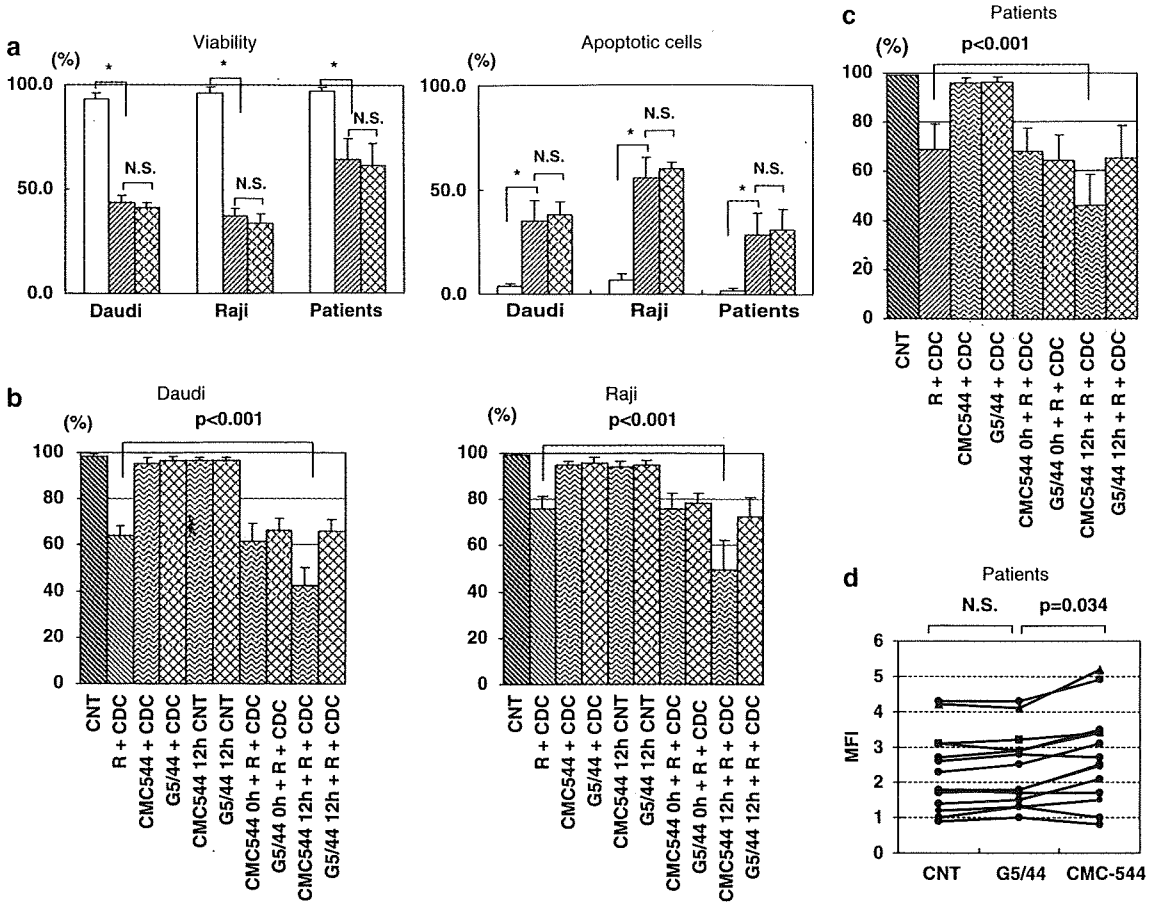

Figure 4 (**a**) Antiproliferative and apoptotic effects were determined by viable cell counts and cell cycles, respectively. These were analyzed after incubation with either rituximab (blank column) or CMC-544 (shaded column) or with both agents (mesh column) and then compared before the incubation. *$P<0.001$, NS: not significant. (**b**) The CDC effect of rituximab in Daudi and Raji cells cultured with or without CMC-544. The viable cell counts after CDC assay were compared with before, and are represented as the rate of percent (%). The viable cell count significantly decreased after rituximab treatment as a result of CDC. It was significantly enhanced by incubation in a CMC-544-free medium for 12 h after exposure to CMC-544. (**c**) The CDC effect of rituximab in cells from 12 patients with BCM cultured with or without CMC-544. The result was similar to that obtained in cell lines. (**d**) After the first 30 min of the CDC assay, cells were placed on ice to stop the reaction and analyzed the compliment deposition on the cells. This was determined by flow cytometry after staining with FITC-anti-human C3c rabbit antibody. MFIs were compared among the groups. Statistical significance is shown in the figure. Black circle, square and triangle show cells from patients, Daudi and Raji cells, respectively.

events occur before and after binding to CD20, the level of CD20 expression is presumed to be an important factor in treatments with rituximab,[3,5] and upregulation of CD20 has been attempted by some investigators.[24] In this study, the level of CD20 was constant or increased 12–24 h following exposure to CMC-544 as analyzed by flow cytometry, and constant by real-time RT-PCR. The preservation of CD20 supports the efficacy of rituximab after treatment with CMC-544.

The levels of CD20 began to decrease over time after 24 h. This might be explained by the direct antiproliferative and apoptotic effects of CMC-544, which started 24 h after incubation with CMC-544. A similar observation was reported in our study of GO.[15,19,20]

Although the level of CD20 mRNA did not change as determined by RT-PCR, the levels of CD20 surface antigen increased as determined by flow cytometry in some samples. This discrepancy might be explained by the increase in cell volume associated with cell cycle events such as calicheamicin-induced transient G2/M arrest.[15] The increase was confirmed by microscopic inspection and scatter-grams of flow cytometry.

The levels of CD22 are also important in the action mechanism of CMC-544 because CD22 directly reacts with mAb moiety of CMC-544. In our study, CD22 decreased 12 and 24 h after CMC-544 exposure as measured by RT-PCR and flow cytometry, respectively. The level of CD22 did not decrease after G5/44 or GO exposure (data not shown). Therefore, the downregulation of CD22 could be an effect of CMC-544, probably induced by a calicheamicin detached from CMC-544.

CD55 and CD59 are important regulators of CDC in BCM.[6,7] The increase of these antigens is reportedly related to their resistance to rituximab, and the decrease to their susceptibility to rituximab.[21,25] However, the underlying mechanism for the increase of these antigens with respect to the resistance to rituximab has not been well elucidated. Decreasing or inactivating CD55 is an effective idea to restore the therapeutic effect of rituximab.[8] In our present analyses, the level of CD55 significantly decreased 12–24 h after CMC-544 exposure. It is consistent with the observation that CDC from rituximab increased 12 h after incubation with CMC-544. These results may also explain the rationale for the advantage in combination of rituximab and CMC-544. The increase of compliment